Palaeotethys-related sediments of the Karaburun Peninsula, western Turkey: Constraints on provenance and stratigraphy from detrital zircon geochronology

Kersten Löwen[1,*], Guido Meinhold[1], Talip Güngör[2], Jasper Berndt[3]

[1] Abteilung Sedimentologie/Umweltgeologie, Geowissenschaftliches Zentrum der Georg-August-Universität Göttingen, Göttingen, Germany

[2] Department of Geological Engineering, Dokuz Eylül University, İzmir, Turkey

[3] Institut für Mineralogie, Westfälische Wilhelms-Universität Münster, Münster, Germany

*e-mail: kersten.loewen@geo.uni-goettingen.de

Tel.: +49 551 399818

Abstract

Detrital zircon U–Pb geochronology of fifteen Late Paleozoic to Early Mesozoic siliciclastic sandstones from the Karaburun Peninsula in western Turkey determines maximum sedimentation ages, identifies possible source areas, and anchors the study area within the Palaeotethyan realm. Siliciclastic sandstones yielded ages from Triassic to Archean with major input from Palaeozoic to Neoproterozoic sources and very few Mesoproterozoic zircons. The youngest age groups set the new limit of the maximum depositional ages to Late Carboniferous–Early Permian for the Küçükbahçe and Dikendağı formations. Detrital zircons from Triassic sandstones are mainly Neoproterozoic and Palaeozoic in age. Zircons from the Scythian–Anisian Gerence Formation are predominantly Devonian and Carboniferous in age, while also Permian and Triassic zircon grains occur in the Carnian–Rhaetian Güvercinlik Formation. According to the zircon age populations and the data available from possible source regions, the Karaburun siliciclastic sediments, with the exception of two samples from the Dikendağı Formation, record sediment supply from units located at the southern margin of Eurasia during Late Palaeozoic and Early Mesozoic times. This interpretation is in agreement with palaeotectonic reconstructions for the closely related Greek islands of Chios and Inousses. The presence of Devonian accompanied by Carboniferous zircons in some of the Karaburun samples reveals similarities with Karakaya Complex sandstones of the Sakarya Zone in NW Turkey.

Keywords

U–Pb geochronology, Detrital zircon, Sediment provenance, Palaeotethys, Karaburun Peninsula, Turkey

Introduction

The Eastern Mediterranean region is made up of several continental fragments which document a highly geodynamic history. Turkey finds itself in a unique position as it represents a geographical junction point between the Asian and European continents as well as a geological link between Gondwana to the south and Eurasia to the north. From north to south, the major geotectonic units and suture zones in western Turkey are: the İstanbul Zone, Sakarya Zone, İzmir-Ankara Zone, Menderes Massif, Lycian nappes and the Taurides (Fig. 1).

Remnants of oceanic basins record the existence of two major oceanic realms, the Palaeozoic to Early Mesozoic Palaeotethys and (mainly) Mesozoic Neotethys (e.g. Şengör et al. 1984; Stampfli 2000, and references therein). It is a general consensus, that Palaeotethys closed in response to northward drift of the Cimmerian terranes (e.g. Taurides) and the opening of Neotethys to the south (e.g. Stampfli and Borel 2002). The exact timing and polarity of subduction of Palaeotethys, however, remains controversial. Different models have been published during the last decades, proposing either northward subduction under Eurasia (e.g. Stampfli 2000; Stampfli and Borel 2002; Robertson et al. 2004; Okay et al. 2006; Moix et al. 2008), southward subduction beneath Gondwana (e.g. Şengör et al. 1984; Okay et al. 1996; Xypolias et al. 2006, 2008; Akal et al. 2011), or a combination of both (e.g. Robertson and Ustaömer 2009). Uncertainty concerning the Palaeotethyan evolution is mainly because of lack of hard data (e.g. provenance data) for testing the various palaeotectonic models. Chios Island (Greece) and Karaburun Peninsula (W Turkey) are regarded as key areas for understanding the closure history of Palaeotethys. Unlike the high-grade metamorphic units in the surrounding area (e.g. Sakarya Zone, Menderes Massif, Cyclades, Pelagonian Zone and Serbo-Macedonian and Rhodope massifs), the Chios and Karaburun localities exhibit virtually unmetamorphosed Palaeozoic and Mesozoic sedimentary rocks (e.g. Besenecker et al. 1968; Erdoğan et al. 1990; Kozur 1998; Robertson and Pickett 2000; Zanchi et al. 2003; Meinhold et al. 2007, 2008a, b;

Robertson and Ustaömer 2009). For the Late Palaeozoic, some workers place the Chios–Karaburun units along the northern margin of Palaeotethys (e.g. Stampfli 2000; Meinhold et al. 2008b; Moix et al. 2008), while others favor a position along the southern margin of Palaeotethys, i.e. along the northern margin of Gondwana (e.g. Robertson and Pickett 2000; Robertson and Ustaömer 2009; Akal et al. 2011).

Provenance data including detrital zircon U–Pb ages were already published for the islands of Chios and Inousses (Meinhold et al. 2008b; Meinhold and Frei 2008) (Fig. 2). Such data are unavailable for the Karaburun Peninsula, except of a few detrital zircon ages from the Karareis and Küçükbahçe formations mentioned in abstract form only (Rosselet and Stampfli 2003). This study provides detrital zircon U–Pb ages for a provenance study of the siliciclastic successions from the Karaburun Peninsula to constrain their origin and the palaeoposition within the Palaeotethyan realm. Besides that, the detrital zircon ages are also crucial for estimating the maximum age of the (Palaeozoic) sedimentary successions, which has long been a matter of debate.

Geological setting

The Karaburun Peninsula is located in the central, westernmost part of Turkey adjacent to the Aegean Sea (Fig. 1). It is part of the İzmir-Ankara Zone, a suture zone separating continental fragments of Eurasian affinity (e.g. Sakarya Zone to the north) from fragments of Gondwana affinity (e.g. Menderes Massif to the south) (e.g. Okay and Tüysüz 1999; Stampfli 2000; Moix et al. 2008). The Karaburun area has been studied for more than 100 years and was first mapped by Philippson (1911), followed by Kalafatçıoğlu (1961) and more recently by other workers (Erdoğan et al. 1990; Robertson and Pickett 2000; Stampfli et al. 2003; Çakmakoğlu and Bilgin 2006). Based on the current knowledge, the Karaburun units comprise a mélange zone of blocks of black chert and pelagic limestones, ranging in age from Silurian to Carboniferous and poorly dated volcanic rocks embedded in a highly deformed siliciclastic matrix of Early Carboniferous age. Thick, autochthonous Mesozoic carbonate platform units unconformably overlie this mélange zone. However, the interpretation of the Karaburun units and the mélange zone is ambiguous; different models have been proposed for their formation. Kozur (1995, 1998) favor a sedimentary olistostromal origin, whereas Robertson and Pickett (2000) suggest an origin as tectonic mélange and interpret the rocks as an accretionary complex related to Late Palaeozoic subduction including a collisional setting. Yet another model proposed an origin as a Triassic rift-related succession including Palaeozoic and Triassic rocks (Erdoğan et al. 1990, 2000), and in a fourth scenario the mélange is considered as an accretionary complex, which was exhumed and reworked as olistostromes into a fore-arc basin during Late Carboniferous time (Stampfli et al. 2003).

The structurally lowest unit was first defined by Kozur (1998) as Küçükbahçe Formation and crops out in the western part of the Karaburun Peninsula (Figs 2, 3). It is composed of a relatively monotonous alternation of low-grade metamorphosed (turbiditic) sandstones and shales, with intercalations of conglomerates, silt- and mudstones, without any blocks. These sediments have experienced intense folding and shearing and have pronounced schistosity. The Küçükbahçe Formation was long supposed to be of Ordovician (or Cambro–Ordovician) age (Kozur 1998), but based on a detrital zircon study by Rosselet and Stampfli (2003) this age has been revised to Early Carboniferous. The upper clastic part of the mélange was first identified as Dikendağı Formation by Çakmakoğlu and Bilgin (2006) and has been assigned to a Silurian–Carboniferous (Visean) age (Kozur 1995, 1998). In the northern part, the formation is dominated by alternations of shales and coarse- to fine-grained sandstones with very low occurrence of olistoliths (black chert). A more pronounced bedding and large blocks of limestone and folded chert that are enclosed in the matrix rocks characterize the succession in the southwestern part of this formation. Blocks of black chert contain radiolarians, ranging in age from Silurian to Carboniferous and limestone blocks have been dated as Silurian to Early Devonian (Kozur 1997, 1998). The existence of chert and limestone blocks, and very slight schistosity, which suggest a decrease in metamorphic degree are the most distinctive features compared to the lower clastic unit (Küçükbahçe Formation). Within the Dikendağı Formation two small granitoid bodies crop out in the northern part of the Karaburun Peninsula and the contacts were interpreted as intrusive (Erkül et al. 2008; Akal et al. 2011). The age of these bodies was constrained to Early Triassic by a biotite Rb–Sr isochron age of 239.9 ± 2.4 Ma (Ercan et al. 2000) and zircon U–Pb ages of 244.4 ± 1.5 Ma (Ustaömer et al. 2016) and 247.1 ± 2.0 Ma, respectively (Akal et al. 2011). The uppermost part of the mélange, only exposed locally (i.e. at the southern coast area of Gerence Bay, Fig. 2) is named Alandere Formation and is interpreted to be gradational with the Dikendağı Formation (Çakmakoğlu and Bilgin 2006). Robertson and Pickett (2000) consider the Alandere Formation as structurally highest block within the mélange; Erdoğan et al. (1990; 2000) consider this formation as fundament on which a Triassic rift-related succession (Karaburun mélange sensu lato) was deposited. The Alandere Formation is mainly composed of fossil-rich, shallow-water limestones and contains sandstones, conglomerates, shales and chert. The age is well-constrained by biostratigraphic data to Carboniferous (Serpukhovian-Bashkirian) (Erdoğan et al. 1990, 2000).

According to Robertson and Pickett (2000) and Çakmakoğlu and Bilgin (2006), the Palaeozoic rocks are unconformably overlain by a thick sequence dominated by Mesozoic platform carbonates, which make up large parts of the eastern and southern area of Karaburun Peninsula. This succession is of Early Triassic to Late Cretaceous (Campanian–Maastrichtian) age and is subdivided into several units, amongst others the Gerence Formation, İdecik unit, Camiboğazı Formation and Güvercinlik Formation. The Gerence Formation unconformably overlies the Karaburun mélange. At its base, it consists of conglomerates with reworked material of the underlying formations and passes upwards into more carbonate-rich conglomerates. Besides, this unit comprises mainly siliciclastic material and carbonates with tectonically stressed and intensely folded cherts. The age of these rocks has been determined by fossils (ammonites, conodonts, foraminiferas) to be Early Triassic. The Camiboğazı Formation on top of this unit is made up of thick bedded and massive limestones. Based on fossils, the age of this unit has been determined to be Middle–Late Triassic (Ladinian–Carnian) in several studies (e.g. Brinkmann et al. 1972; Erdoğan et al. 1990, 2000). In the upper part of the Mesozoic sequence, these carbonates are gradationally overlain by the Güvercinlik Formation. This is a detritic succession that contains highly mature, red sandstones and conglomerates as well as oolitic and dolomitic limestones (Stampfli et al. 2003; Çakmakoğlu and Bilgin 2006) with abundant megalodon fossils, algae and gastropods of Late Triassic age (Çakmakoğlu and Bilgin 2006). The İdecik unit is thrust between the Karaburun mélange and the Gerence Formation and is only exposed in a small strip in the central part of northern Karaburun Peninsula. It mainly consists of volcanoclastic rocks, basic lavas, tuffaceous material, limestone and radiolarites. According to the red radiolarites from the lower part a Ladinian–Carnian age has been assigned for this unit (Çakmakoğlu and Bilgin 2006).

Methods

Rock samples were collected from outcrop and processed at the Geoscience Center of Göttingen University. Lithology, stratigraphy and geographic coordinates of studied samples are given in Table 1. For U–Pb geochronology, zircons were separated from bulk-rock samples by standard routines: jaw crusher, disc mill, Wilfley table, Frantz magnetic separator and heavy liquid (sodium polytungstate). Final selection of zircon grains was done by handpicking under a stereomicroscope. The zircons were fixed in epoxy resin mounts and polished to expose the interior of the grains. Prior to the analyses, cathodoluminescence (CL) imaging was applied to reveal their internal structures (e.g. growth zones) and to guide spot placement. The U–Pb age determination was performed on a sector-field ICP-MS (Element2, ThermoFisher) coupled to a 193-nm Analyte G2 Excimer Laser Ablation System. Laser spot size was commonly 35 µm, but was reduced to 25 µm in some cases to analyze thin overgrowths. Isotope data were acquired on masses 202, 204, 206, 207 and 238. The mass 202 was used to quantify interference of ^{204}Hg on ^{204}Pb. Common Pb correction was only applied to an analysis if the fraction of common ^{206}Pb to total ^{206}Pb exceeded 1%. Mass discrimination and elemental fractionation during laser ablation were corrected by bracketing 10 unknown samples by 3 measurements of the GJ-1 reference zircon (Jackson et al. 2004). To keep track of precision and reproducibility of U–Pb ages, the 91500 reference zircon (^{206}Pb/^{238}U = 1062.4 ± 0.8 Ma; ^{207}Pb/^{206}Pb = 1065.4 ± 0.6 Ma; Wiedenbeck et al. 1995) was analysed in the course of this study. Measured isotopic ratios matched the published values of Wiedenbeck et al. (1995) within error.

Data reduction was done following the procedure described by Kooijman et al. (2012). Given the natural break in U–Pb ages between ca. 800 and 1200 Ma the data were filtered based on two criteria: accepted were all zircon ages a) within 90–110% concordance [100 × (^{206}Pb/^{238}U / ^{207}Pb/^{206}Pb)] for grains older than 1200 Ma and b) grains showing a difference of the U–Pb ages in the range of 10% for ages younger than 1200 Ma (see also Allen and Barnes 2006; Spencer et al. 2014). By this means we want to account for low precision of ^{207}Pb/^{206}Pb values for younger (<1200 Ma) ages. ^{206}Pb/^{238}U ages were quoted for zircons younger than 1200 Ma, and ^{207}Pb/^{206}Pb ages to depict zircons older than 1200 Ma (Gehrels et al. 2008). This age was chosen because there is a natural gap in the ages of zircons in the analysed samples.

Concordia plots (Fig. 5, 7, 9) were produced with Isoplot version 3.75 (Ludwig 2003) and kernel density estimates and histograms (Fig. 6, 8, 10, 12) were produced using the DensityPlotter software by Vermeesch (2012). The analytical data are given as electronic supplementary material (Table S1). The geological time scale GTS of Gradstein et al. (2012) was used as stratigraphic reference for data interpretation.

Results

We present the detrital zircon U–Pb ages for each of the studied formations in upward order in the tectonostratigraphy, first for the Triassic, followed by the Palaeozoic, because the stratigraphic ages of the youngest formations are well constrained by biostratigraphic data (Fig. 3), while the ages of the older formations are a matter of debate.

Gerence Formation

From the Gerence Formation, one sample (KAR1) was collected near the west coast of Karaburun at Gerence Bay (Fig. 2). The sample is a coarse-grained feldspar-rich litharenite which consists of mainly quartz and abundant chert, plagioclase and lithic fragments of volcanic and sedimentary origin. Many grains are cut by carbonate veins. The zircon population is commonly subhedral and has oscillatory zoning patterns. A total of 59 spots on 56 zircon grains were analysed and filtered data (n = 51; Fig. 6a) show a unimodal age distribution with a well-defined population at 350–400 Ma (n = 24). More than 50% of the zircons are of Devonian age and only a single analysis yielded a Mesoproterozoic age (ca. 1140 Ma), which marks the upper end of the spectrum. The youngest age group (n = 3, analyse numbers (#): 23, 39, 45) occurs at 330–345 Ma including the youngest grain (#: 39) of 334 ± 7 Ma that indicates a late Early Carboniferous maximum depositional age.

İdecik unit

From the İdecik unit, two samples were collected in close distance to the Dikendağı Formation near the Gerence Bay in western Karaburun (Fig. 2). Sample KAR3 is a coarse-grained sublitharenite dominated by monocrystalline quartz with minor amounts of feldspar, muscovite and lithic fragments of mainly volcanic and (meta)sedimentary origin. In general, the zircon grains are well rounded but some euhedral grains are also present. Most of them have oscillatory zoning and a small number exhibit xenocrystic cores. U–Pb ages were obtained from 104 spots on the same number of grains, resulting in 81 accepted zircon ages (Fig. 6b). The age spectrum ranges from ~230 Ma to 2.75 Ga and is dominated by Proterozoic zircons (ca. 70%).

Two major age groups occur at ca. 500–550 Ma (*n* = 8), and 650–750 Ma (*n* = 15). Minor populations exist at 900–1000, 1950 and 2500 Ma. The youngest apparent age is 234 ± 5 Ma, but belongs to a high U- (1072 ppm) and common Pb-bearing (3.25%) crystal and is therefore not considered as reliable indicator for the maximum age (#: 89). Another single grain yielded an age of 313 ± 5 Ma (#: 126), however, the youngest coherent age group (*n* = 4, #: 69, 92, 106, 117) occurs at 450–470 Ma.

Sample KAR4 is a fine-grained litharenite that predominantly consists of mono- and polycrystalline quartz and volcanic and (meta)sedimentary lithoclasts. Small amounts of feldspar, muscovite, chlorite and carbonate are also present. The dataset comprises 96 analyses from 94 zircon grains. These are generally well rounded or short prismatic, and CL images revealed oscillatory zoning and irregular patterns. Filtered data (*n* = 80) indicate a bimodal age spectrum from ca. 330 Ma to 2.7 Ga (Fig. 6c). A major Cambrian age group occurs at ca. 510 Ma and a second group exists at ca. 2.0 Ga. The input of Palaeozoic zircons (ca. 55%) is much higher compared to sample KAR3. The maximum age of deposition is indicated by the youngest group (*n* = 4, #: 145, 183, 186, 206) of coherent zircons between 330 and 345 Ma.

Güvercinlik Formation

Two samples (KAR20A and KAR20B) of the Güvercinlik Formation were collected from an outcrop at the eastern coast of Karaburun, ca. 4 km north of Balıklıova (Fig. 2). KAR20A is a highly mature coarse-grained quartz arenite. KAR20B is a (detrital garnet-bearing) sublitharenite. Both samples almost purely consist of quartz. The zircon population of both samples consists of mainly colorless to pinkish, euhedral grains with oscillatory zoning patterns. For sample KAR20A, 110 spots on 85 grains were analysed of which 103 U–Pb ages were accepted. The total spectrum ranges from 200 Ma to 2.6 Ga with a distinct Mesoproterozoic age gap and a major input of Palaeozoic, especially Carboniferous zircons (Fig. 6d). Three distinct groups occur at ca. 320 Ma, ca. 510 Ma and ca. 1.9 Ga, respectively. The youngest grain occurs at 202 ± 4 Ma (#: 291), whereas the youngest age group is defined by three zircons (#: 271, 274, 308) at ca. 235–245 Ma. The dataset of sample KAR20B comprises 104 spots on 87 zircon grains. Filtered data (*n* = 94) vary between 200 Ma and 1.0 Ga, with a single spot age at 2.0 Ga (Fig. 6e). Of the Palaeozoic zircons, Carboniferous ages (*n* = 35) are most common and define a prominent group at 330 Ma. The youngest coherent group (*n* = 3, #: 386, 391, 395) is of latest Triassic age (ca. 202 Ma). It is worth mentioning that these grains exhibit large amounts of common ^{206}Pb (2–10%).

Küçükbahçe Formation

The Küçükbahçe Formation is one of the main siliciclastic units and was therefore studied in detail. Four samples were collected from different locations of the formation to obtain a representative overview. Sample KAR9 is a fine-grained sublitharenite made up of monocrystalline quartz and small amounts of feldspar and muscovite from a location ca. 1 km west of Küçükbahçe village (Fig. 2). From this sample, 79 spots on 70 grains were analysed, of which 64 U–Pb ages were accepted. The grains are subhedral and smaller grains are well rounded with mainly oscillatory zoning and occasional homogenous CL patterns. The data define a polymodal age spectrum between 250 Ma to 3.0 Ga with an age gap between 1.2–1.8 Ga and prominent peaks at ca. 320 Ma and ca. 630 Ma (Fig. 8a). Minor peaks occur at ca. 840 Ma and 1.95 Ga. The lower end of the spectrum is defined by a single spot age of 248 ± 4 Ma from an U-rich (2496 ppm) and common Pb-bearing (2.76%) grain that is not considered as geologically meaningful. A group (*n* = 5, #: 427, 447, 448, 460, 470) of zircons at 310–325 Ma indicates the maximum age of deposition.

The second sample (KAR10), a fine-grained subarkosic rock is from the central part of the unit and is texturally similar to the previous one. Well-rounded grains with diverse, often chaotic or homogenous CL patterns characterise the zircon population. The zircon data comprise 83 spots on 75 grains and the filtered data (*n* = 65) are dominated by Neoproterozoic U–Pb ages (ca.

50%) (Fig. 8b). The spectrum is comparable to sample KAR9 and ranges from ca. 300 Ma to 3.0 Ga with an age gap between 1.2 to 1.8 Ga. Several age groups are present at ca. 300–350 Ma, ca. 550–600 Ma and ca. 975 Ma of which the youngest group (*n* = 3, #: 481, 503, 535) indicates a maximum age of deposition of Pennsylvanian–Cisuralian.

Sample KAR11 is a feldspathic litharenite that was collected from the northern part of the study area, ca. 4 km SW of Yeniliman village (Fig. 2). This sample mainly consists of quartz, plagioclase, K-feldspar, muscovite and predominantly metasedimentary fragments in a very fine-grained matrix. Although some zircon grains are euhedral to subhedral, most of them are rounded. CL images revealed that xenocrystic cores are common and many grains have disturbed patterns. Filtered data comprise 88 zircon ages from 109 spots measured on 103 grains. Zircon ages range from 300 Ma to 3.0 Ga and define two major groups at 350–450 Ma and 500–650 Ma (Fig. 8c). Two smaller groups occur at ca. 1.8 and ca. 2.6 Ga. The youngest single spot ages (#: 588, 612) are 307 ± 15 and 318 ± 14 Ma, but the maximum depositional age is constrained by a group (*n* = 3, #: 559, 598, 626) of coherent U–Pb ages at ca. 345–360 Ma.

A fourth sample (KAR27), classified as sublitharenite was collected from the eastern central part of the unit, close to the Dikendağı Formation (Fig. 2). It predominantly consists of monocrystalline quartz and lithic fragments with some feldspar and mica. The majority of the zircon grains are subhedral or well rounded and CL images show oscillatory zoning and xenocrystic cores surrounded by younger rims. Filtered zircon ages (*n* = 50) result from analyses of 57 spots on the same number of grains and show a polymodal age distribution with a major group (*n* = 9) at 350–400 Ma (Fig. 8d). Minor populations exist at ca. 625 Ma, ca. 875 Ma, ca. 1.0 Ga and ca. 2.0 Ga. Proterozoic zircons make up 50% of the data and Devonian to Carboniferous grains dominate the Paleozoic age group. Two single grains (#: 657, 663) yielded Cisuralian ages and the youngest group of coherent zircon ages (*n* = 4, #: 651, 659, 662, 675) occurs at 330–340 Ma, defining the upper limit for deposition.

Dikendağı Formation

The second main clastic unit of inferred Palaeozoic age is the Dikendağı Formation from which five samples were analysed. Samples KAR5 and KAR6 were collected from the southern part of this formation within a close distance (ca. 2 km). Both sediments are fine-grained sublitharenites with similar mineral assemblages of quartz, feldspar, muscovite and chlorite. Their zircon populations are dominated by well rounded, colorless to pinkish grains with various, oscillatory zoning, homogenous or chaotic CL patterns. The dataset of sample KAR5 comprises 109 spots on 106 grains of which 90 U–Pb ages between ca. 330 Ma and 2.9 Ga were accepted. A prominent group occurs at 550–650 Ma (Fig. 10a) and several smaller groups exist between 850 Ma and 1.1 Ga and 1.7–2.1 Ga, respectively. One single spot age (#: 688) at 334 ± 7 Ma defines the lower limit of the spectrum, but the maximum age of sedimentation is indicated by a group of zircons (n = 3, #: 740, 757, 761) at 550–565 Ma. For sample KAR6, 62 spots on 52 grains were analysed. Filtered zircon ages (n = 47) show a polymodal age distribution ranging from 200 Ma to 2.0 Ga. Major groups occur at 300–400 Ma and 550–600 Ma (Fig. 10b) and additional age groups appear at ca. 750–800 Ma and 850–900 Ma. The youngest three single spot ages are Permian and Triassic (#: 778, 785, 797) including a high common Pb-bearing (4.56%) Upper Triassic grain which is not considered to be geologically meaningful. A group (n = 8, #: 774, 775, 783, 787, 789, 790, 804, 810) of grains within the range of 300–350 Ma define the maximum age of sediment deposition. Mesoproterozoic zircons are, except of two grains at ca. 1.0 Ga completely absent, but a small amount of Paleoproterozoic grains exists.

A third sample (KAR7) from the southern area was classified as a lithic arkose and is characterised by highly abundant and large feldspar crystals and lithic fragments. The U–Pb zircon data consist of 134 spots on 127 grains, of which 126 ages were accepted. These grains are colorless to light orange and of subhedral to euhedral shape with predominantly oscillatory zoning patterns. Most of the zircons (ca. 90%) are of Paleozoic age and define a single, Early Palaeozoic peak at 400–450 Ma (Fig. 10c). Although the youngest single spot ages occur at 294

Ma and 308 Ma (#: 833, 841), the maximum age of deposition is constrained by a group (*n* = 5, #: 836, 852, 857, 906, 938) of zircons between 370 and 385 Ma.

Sample KAR14 was collected ca. 2 km southeast of Yeniliman village (Fig. 2). It is a subarkosic sediment dominated by monocrystalline quartz and to some extend feldspar within a muscovite-bearing matrix. In most cases, the zircon grains are light pinkish and well rounded with oscillatory growth zoning. In total, 72 spots were analysed on 65 grains and filtered data contain 61 U–Pb ages. Except of two, they are all Proterozoic or older in age and show a distribution pattern characterized by two broad groups at 550–700 Ma and 900–1100 Ma (Fig. 10d) and a smaller peak at 1.85–1.9 Ga. A group of Ediacaran-aged zircons (*n* = 6) between ca. 550 and 570 Ma marks the maximum age of sedimentation for this sample.

One last sample (KAR15) was taken from a location close to the contact to the Early Triassic granitoid intrusions in northern Karaburun. The sediment is classified as quartz arenite and thus, predominantly consists of quartz with only small amounts of feldspar, muscovite and chlorite. Lithic fragments are virtually absent. From this sample, 22 grains were analysed on 27 spots, of which 23 were accepted. Zircon grains are well rounded and of euhedral shape, in similar abundance, and have oscillatory zoning patterns and rare xenocrystic cores. The ages range from ca. 340 Ma to 2.7 Ga with main groups at 350–400 Ma and 500–550 Ma (Fig. 10e).

Alandere Formation

For the Alandere Formation, one sample (KAR22) was collected from a location at the southern coast of Gerence Bay (Fig. 2). The sediment is a coarse-grained, garnet-chromite-bearing subarkosic rock consisting of primarily quartz and feldspar with lithic fragments of mostly volcanic origin. The most zircon grains are colorless to light pinkish and have a subhedral shape with oscillatory zoning patterns. For this sample, 88 spots on 73 grains were analysed. Of these, 73 zircons met the filtering criteria and yielded U–Pb ages between 280 Ma and 2.7 Ga with very few zircons from 800 Ma to 1.8 Ga (Fig. 10f). One major age group (*n* = 13) exists at 350–400

Ma and three smaller peaks occur at ca. 520, ca. 620 and ca. 720 Ma. The youngest small group (*n* = 2, #: 1034, 1047) of zircons occurs at ca. 330 Ma but a larger coherent group (*n* = 6, #: 1029, 1031, 1045, 1051, 1071, 1097) exists at 357–370 Ma and is considered to indicate a Carboniferous (Mississippian) maximum depositional age. The Permian and Late Carboniferous single spot ages (#: 1033, 1076) at ca. 280 Ma and 310 Ma are due to their high U and common Pb content not considered for further interpretation.

Discussion

Maximum depositional ages and revised stratigraphy

Age spectra of detrital zircons from sedimentary rocks provide provenance information as well as constraints for the timing of sediment deposition (e.g. Fedo et al. 2003). In case of the Karaburun Peninsula the depositional ages of the Mesozoic sequences were already well defined by biostratigraphic data. However, the age of the underlying Palaeozoic clastic rocks was only loosely constrained and stratigraphic correlations were interpreted in different ways (e.g. Erdoğan et al. 1990, 2000; Çakmakoğlu and Bilgin 2006). Based on our results, we present new evidence for the timing of sediment deposition and review previously published stratigraphic models (Fig. 3). Compiled information on the stratigraphic age of the different formations of Karaburun Peninsula inferred from fossils and the depositional age according to new U–Pb detrital zircon data are given in Table 1.

The Güvercinlik Formation represents the highest structural and stratigraphic level of the investigated sediments. Two samples (KAR20A and KAR20B) yielded consistently similar distribution of zircon ages (Fig. 11), including one grain of ca. 202 Ma in the first sample but three more latest Triassic zircons in the latter. As the sample locations are in close proximity and their chemical and petrographic characteristics are matching, the youngest group extracted from the combined dataset, probably indicates the maximum age of sediment deposition, thus confirming the data of Erdoğan et al. (1990, 2000) and Çakmakoğlu and Bilgin (2006). An Early Triassic age has been assigned to the Gerence Formation based on biostratigraphic data: the youngest group of zircons from this study is Visean, which provides the maximum age of deposition for this succession based on U–Pb geochronology. This could be a result of a low zircon count (*n* = 51), which might be insufficient to detect every population that was present in the sample. Another more likely explanation implies that rocks of Early Triassic age were either never present or not yet exposed in the source area at the time of deposition. A similar scenario could explain the situation for the İdecik unit. Çakmakoğlu and Bilgin (2006) assigned a Ladinian–Carnian age to this unit whereas results from U–Pb dating indicate an Early Carboniferous depositional age. The age distribution pattern of one of the samples (KAR4) shows striking similarities to the late Palaeozoic Küçükbahçe Formation (Fig. 11). This suggests, recycling of these rocks could have provided large amounts of detritus for the İdecik unit or both were supplied by the same source.

Information on the siliciclastic rocks that make up large parts of the northern and western area of Karaburun Peninsula is scarce. Erdoğan et al. (1990) introduced the term Karareis Formation to describe the clastic sequences in northwestern Karaburun and interpreted the carbonate-rich Gerence Formation in the southwestern and eastern part as a lateral equivalent of the Karareis Formation. Both were assigned to the so-called Denizgiren Group of assumed Scythian–Anisian age (Fig. 3). Later, these detrital sequences to the west were considered as separate units: (1) the Küçükbahçe Formation for which an Ordovician (or Cambro–Ordovician) deposition was suggested and (2) the Dikendağı Formation of assumed Silurian–Carboniferous age (Visean) (Kozur 1998; Çakmakoğlu and Bilgin 2006) (Fig. 3). Some Visean zircons have been mentioned for the Küçükbahçe Formation in an abstract by Rosselet and Stampfli (2003), but here we present the first extensive U–Pb dataset of detrital zircons from the siliciclastic units. Our results comprise more than 600 single zircons and clearly indicate a considerably younger depositional age for both formations, which is in marked difference to previously published data (Fig. 3). The maximum age of deposition for the Küçükbahçe Formation is constrained by a group (n = 11) of Pennsylvanian–Cisuralian zircons extracted from the combined dataset of all samples. Filtered data from the Dikendağı Formation contain less (n = 7) grains of Late Carboniferous–Early Permian age, almost exclusively from samples (KAR5, KAR6, KAR7) collected from the southern part of the formation. According to the zircon spectra alone, samples from the northern region could have a slightly older, probably Lower Devonian–Early Carboniferous maximum depositional age. This could also be an effect of the smaller data base for the northern part (n = 84) or refer to one of the reasons given below. Nevertheless, we consider this as sufficient indication for time equivalent deposition of both formations. Regarding the Dikendağı Formation, the minimum age of sedimentation is defined by an Early Triassic (247 ± 2.0 Ma, Akal et al. 2011; 244.4 ± 1.5 Ma, Ustaömer et al. 2016) granitoid intrusion in the northern part of the peninsula. During fieldwork, an unknown mafic intrusion was discovered in the northwestern part of the Küçükbahçe Formation that may also provide a lower limit of sediment deposition (Fig. 13); a geochronological study is underway. With respect to the zircon spectra, the Küçükbahçe Formation is characterised by notably consistent age distribution with only little variation (Fig. 11). On the contrary, the supposed time equivalent Dikendağı Formation shows distinct heterogeneity with respect to, not only zircon distribution, but also petrography and chemical composition (Löwen and Meinhold, unpublished data). This may have several reasons: (1) It is the result of provenance change through time; (2) Field observations reveal that the lithology of the northern and southern part of this unit is variable; large chert and limestone blocks are restricted to the south only. Nonetheless, the entire area is mapped as a single formation but possibly needs further subdivision; (3) Above listed differences correspond to distal and/or proximal extensions of turbidity currents. (4) Some of the analysed samples could have been part of larger blocks (probably olistolithes) that are enclosed in the matrix rocks and do not represent the matrix itself. Future studies might solve the issue of heterogeneity within the Dikendağı Formation.

For the Alandere Formation our zircon results are in good agreement with the previously assigned Serpukhovian–Bashkirian age. These findings allow refinement of the current stratigraphy and regional correlations of the Palaeozoic units (Figs. 3, 13). New data indicate that sediment accumulation of the Küçükbahçe and Dikendağı formations did not start in Ordovician (or Cambro-Ordovician) time but most probably began in the mid-Carboniferous and continued to at least Pennsylvanian–Cisuralian. This implies that the Alandere Formation, until now interpreted as youngest section of the mélange (Robertson and Pickett 2000), represents the oldest and therefore lowermost part of the mélange (see also Erdoğan et al. 1990). In the light of these findings, a supposed gradational contact with the Dikendağı Formation and its stratigraphic position seems questionable. Besides, the Küçükbahçe Formation and overlying Dikendağı Formation were also thought to be separated by a gradational contact. However, as both units, to some extent, exhibit very similar lithologies but have different provenance and show different metamorphic overprint, we favor a tectonic contact in agreement with Robertson and Ustaömer (2009). Thus, the previously construed Ordovician–Carboniferous sedimentary sequence is rather a pile of units deposited in Carboniferous–Early Permian times. Combined new data and indications from field work suggest that the present-day stratigraphic order was established by westward thrusting, not before Cretaceous times.

Similar Palaeozoic rocks that are comparable to the mélange zone of Karaburun occur on the neighboring islands of Chios and Inousses in the eastern Aegean Sea (Fig. 2). Chios is tectonostratigraphically subdivided into an ‘autochthonous’ Lower Unit including a Carboniferous mélange and Mesozoic carbonates and a tectonically overlying ‘allochthonous’ Upper Unit of Late Carboniferous to Jurassic age (Besenecker et al. 1968; Meinhold et al. 2007; 2008b) (Fig. 3). The Lower Unit consists of Late Palaeozoic siliciclastic rocks including blocks of limestone, radiolarites and volcanic rocks of Silurian to Carboniferous age and shows striking similarities to the block-bearing Dikendağı Formation of Karaburun (e.g. Robertson and Ustaömer 2009). This (supposed) relation is further underlined by the refined stratigraphic section and indicates that this succession may represent a Late Carboniferous–Early Permian equivalent of the Chios mélange.

On Inousses Island, low-grade metasedimentary rocks are subdivided into two lithostratigraphic units (Besenecker et al. 1971; Kilias 1987; Meinhold et al. 2007). The Lower unit mainly crops out as small patches in the southern part of the island and consists of psammitic rocks with conglomeratic layers. The Upper Unit is made up of pelitic to psammitic rocks and covers the northern part including a small area on the NE tip of Chios that is interpreted as part of Inousses (Kauffmann 1965; Besenecker et al. 1968; Besenecker et al. 1971). The whole sequence is of a monotonous character and does not contain fossils or specific marker horizons for certain stratigraphic correlations. Some workers assigned the metasedimentary succession of Inousses to Permian–Triassic rocks of the Pelagonian Zone of continental Greece and the Sporades Islands (Mountrakis et al. 1983; Kilias 1987). In contrast, Kozur (1998) correlated the Inousses clastic rocks with the Küçükbahçe Formation of the Karaburun Peninsula to the east, for which he suggested an Ordovician (or Cambro–Ordovician) age. Meinhold and Frei (2008) constrained the maximum age of deposition to be Late Carboniferous by dating of detrital zircons. Based on field observations and provenance data, the metasedimentary rocks of Inousses are correlated with the Küçükbahçe Formation; a Pennsylvanian–Cisuralian depositional age is suggested (this study). A comparison of age spectra from both successions reveals congruent distribution patterns, characterised by a predominance of 300–700 Ma-old zircons and minor groups between 1.7–2.2 Ga and 2.45–2.8 Ga as well as a lack of 1.1–1.7 Ga-old zircon grains (Fig. 12). In addition to the zircon data, petrographic observations and geochemical analysis of the sediments of Küçükbahçe Formation reveal great similarities to those from Inousses (Löwen and Meinhold, unpublished data).

Provenance

Our samples derive from different stratigraphic levels and cover a time slice from Late Palaeozoic to latest Triassic. The zircon age distribution of these rocks reflects the entirety of zircon from exposed rocks at the time of sediment deposition and therefore is a powerful tool to identify possible source region(s).

In recent times, several studies have been performed on detrital zircons of Palaeozoic siliciclastic rocks from the larger study area that provide important references for the provenance of the Karaburun sediments. In the Menderes Massif of the western Taurides Neoproterozoic basement rocks are covered by lower Palaeozoic platform sediments. Zircon age spectra from the lower part of this cover are dominated by Neoproterozoic zircons with generally negative εHf values and reveal striking similarities to Cambrian–Ordovician sandstones from Israel and Jordan. The patterns were interpreted to tie the Menderes Massif to the Afro-Arabian margin of northern Gondwana in lower Palaeozoic time (Zlatkin et al. 2013). Similar Palaeozoic to Triassic sedimentary cover rocks crop out in the Karacahisar dome of the Taurides (south-central Turkey). U–Pb zircon data reveal a predominant Neoproterozoic zircon population in Cambrian–Ordovician sandstones and were linked to sediments from Afro–Arabia of the same age as well (Abbo et al. 2015). Furthermore, zircon spectra of the Triassic sequence lack evidence for any post-Cambrian or Variscan sources and suggest that the Tauride domain remained in close proximity to northern Gondwana and did not detach until Middle–Upper Triassic time (Abbo et al. 2015). A study on the Palaeozoic evolution of the northern Gondwana continent was carried out by Meinhold et al. (2011) in the eastern Murzuq Basin of southern Libya. Analysed Palaeozoic and Mesozoic sandstones of this basin cover the Archean to Proterozoic rocks of the Saharan Metacraton. Detrital zircons from the Palaeozoic and Mesozoic sandstones revealed similar age spectra with four main populations of early Proterozoic–Neoarchean, Paleoproterozoic, Stenian–Tonian and Cryogenian–Ediacaran age with variable abundance. Zircons of the pre-Paleoproterozoic age groups were assigned to basement rocks of the underlying Saharan

Metacraton, whereas the younger Cryogenian–Ediacaran grains were related to orogenic events affecting northern Gondwana. The provenance of the Stenian–Tonian population is not yet clarified, but zircons could have been derived either from igneous rocks from areas south(east) of Libya or represent recycled detritus from Neoproterozoic sediments (Meinhold et al. 2011). An extensive dataset has also been established for late Palaeozoic siliciclastic rocks of the External Hellenides. Detrital zircon spectra obtained from rocks of the Phyllite-Quartzite Unit from Crete, Kythera and the Peloponnesus (Chatzaras et al. 2016; Marsellos et al. 2012; Zulauf et al. 2016) are characterised by a prominent Neoproterozoic population with significant input of Ediacaran and Stenian/Tonian proportions. Based on these similarities and the lack of Ordovician to Triassic zircons, combined with a Mesoproterozoic age gap these rocks were interpreted as time and facies equivalent sequences, deposited along the northern margin of Gondwana, isolated from Variscan sources (Chatzaras et al. 2016). In contrast, Early Permian quartzites from the pre-Alpine basement and cover rocks of the lower Tyros Unit on Crete record distinct influx of Variscan detritus (50–70% Carboniferous/Permian detrital zircons) suggesting deposition in close proximity to the southern active margin of Eurasia (Zulauf et al. 2015).

In case of the Karaburun samples the overall zircon data comprise a wide range of ages from 202 Ma to 3.0 Ga thus reflecting various stages of crustal growth and/or recycling. Common features of the population are several groups of Palaeozoic to Neoproterozoic zircons, a very low number or even lack of zircons from 1.2–1.7 Ga and the presence of smaller populations at ca. 1.7–2.2 Ga and/or ca. 2.5 Ga, respectively. These attributes clearly exclude Amazonian (west Gondwana) or Baltican provenance as Mesoproterozoic zircons are widespread in these regions and would have been recorded in their erosional products. For the purpose of our study – identifying possible source regions – the Early Neoproterozoic and older zircons are not necessarily useful to pinpoint a certain area as those ages come up in nearly all samples and may have a variety of sources. A more promising approach focuses on the distribution of Late Neoproterozoic (ca. 540–650 Ma, i.e. ‘Pan-African/Cadomian’) and Palaeozoic (ca. 280–330 Ma, ca. 370–400 Ma, ca. 430–460 Ma, ca. 480 Ma) potential igneous source rocks since they are important time-markers for palaeotectonic reconstructions in the Eastern Mediterranean (e.g. Meinhold et al. 2008b) (Fig. 14).

The large input of zircons from 650–540 Ma is most probably related to the Pan-African and Cadomian orogenies. Both events were linked to the formation of the Gondwana supercontinent in Late Neoproterozoic time. Whereas the term ‘Pan-African’ orogeny generally refers to the cratonic domains (continent–continent collision) and the Cadomian domain (Avalonian–Cadomian belt) is interpreted as peripheral or accretionary orogenic belt that assembled at the northern margin of Gondwana and was accompanied by subduction-related magmatism (Nance and Murphy 1994; Windley 1995). Detrital and magmatic zircons of Late Neoproterozoic age (Pb–Pb, U–Pb) have been published for several terranes in the Eastern Mediterranean region: Menderes Massif (e.g. Sandıklı, Çine and Ödemiş submassifs) in western Turkey (Kröner and Şengör 1990; Hetzel and Reischmann 1996; Hetzel et al. 1998; Loos and Reischmann 1999; Gessner et al. 2004); İstanbul Zone in northern Turkey (Chen et al. 2002; Ustaömer et al. 2005); Kraiste region in Bulgaria (von Quadt et al. 2000; Graf 2001; Kounov 2002); Serbo-Macedonian Massif in northern Greece (Himmerkus et al. 2006, 2007) (Fig. 14).

A group of two samples from the Gerence Formation (KAR1) and Dikendağı Formation (KAR7) reveal unimodal age spectra in the range of 350–450 Ma and 400–500 Ma, respectively (Fig. 6a and 10c). These patterns clearly indicate sediment supply from localised sources of Ordovician to Devonian age. In case of the Ordovician zircons, these rocks are restricted to very few regions only. Possible source rocks are located in the Sakarya Zone from which Özmen and Reischmann (1999) reported Middle Ordovician (462 ± 6 Ma) ages for basement rocks of the Biga Peninsula; smaller metagranitic bodies occur in the Tavşanlı Zone (467 ± 5 Ma, Okay et al. 2008; 446 ± 8 Ma, Özbey et al. 2013) (Fig. 14). Similar ages are also known from granites and gneisses of different parts of the Balkan region, such as the Sredna Gora Zone and Serbo-Macedonian Massif (Titorenkova et al. 2003; Peytcheva and von Quadt 2004; Carrigan et al.

2005) (Fig. 14). Large volumes of possible Silurian orthogneisses make up the basement of the Vertiskos Unit of the NW Serbo-Macedonian Massif (Himmerkus et al. 2006, 2007, 2009a; Meinhold et al. 2010). The above-mentioned areas exhibit suitable source rocks and may have provided large volumes of detritus for the siliciclastic rocks of Karaburun.

Early Devonian igneous rocks are well documented from different parts of the Sakarya Zone (Fig. 14). Zircon U–Pb ages of ca. 395 Ma have been reported for the Karacabey Pluton (Sunal 2012) and similar Pb–Pb ages were obtained from metagranodiorite and gneisses of the Biga Peninsula (Okay et al. 1996, 2006). Magmatic rocks of Carboniferous to Early Permian age ('Variscan') are very common and widespread in the Eastern Mediterranean region and have been reported from the External Hellenides, the Cycladic islands, the Kazdağ Massif of the Sakarya Zone and several parts of the Rhodope Zone (e.g. Engel and Reischmann 1998; Reischmann 1998; Özmen and Reischmann 1999; Keay et al. 2001; Xypolias et al. 2006; Anders et al. 2007; Turpaud and Reischmann 2010; Zulauf et al. 2015). They record a major magmatic phase during that period which was related to subduction and closure of Palaeotethys (Pe-Piper and Piper 2002).

Studied rocks from the Mesozoic part of the Karaburun Peninsula are of Early to Late Triassic stratigraphic age but only samples of the Güvercinlik Formation document sediment supply from (Permian)–Triassic sources. These ages are not common for domains of the N-African continent but Triassic magmatic activity has been recognised in many places of the Eastern Mediterranean region. Such zircons are most likely related to the Serbo-Macedonian Massif, the Pelagonian Zone, the Cycladic islands, the External Hellenides and/or the Menderes Massif from which U–Pb and Pb–Pb data have been reported (e.g. Tomaschek et al. 2001; Koralay et al. 2001; Bröcker and Pidgeon 2007; Anders et al. 2007; Himmerkus et al. 2009b; Zulauf et al. 2015).

As aforementioned detrital zircon of Palaeozoic to Triassic sediments from parts of the Taurides (Menderes Massif, Karacahisar) and External Hellenides (Crete and Peloponnesus) revealed significant differences between terranes that were placed either at the southern Eurasian or northern Gondwana margin (Abbo et al. 2015; Chatzaras et al. 2016; Zlatkin et al. 2013; Zulauf et al. 2015, 2016). The latter were generally characterised by large Cambrian and Neoproterozoic populations with low amount of Palaeozoic zircons (e.g. Karacahisar dome and Menderes Massif), whereas widespread occurrence of Carboniferous to Permian zircons (e.g. pre-Alpine basement on Crete) was attributed to Variscan sources. Even though our samples exhibit prominent Neoproterozoic populations as well, the available information and indicative Palaeozoic age groups – Ordovician–Devonian in particular – clearly support terranes north of the present location of our study area as most likely sources for the Karaburun, Chios and Inousses sediments. In terms of palaeogeography we propose a location in close proximity to the Sakarya, Pelagonian and/or Rhodope zones, or equivalent rock units not present anymore due to erosion and/or subduction, definitely at the southern margin of Eurasia in Late Palaeozoic time (see also Meinhold and Frei 2008; Meinhold et al. 2008b) (Fig. 15). Carboniferous foraminiferal fauna of the Chios–Karaburun units, which show distinct biogeographical affinities to the southern Laurasian shelf (Kalvoda 2003), support this. However, the above-mentioned statements do not seem to be valid for two samples from the Dikendağı Formation (KAR5 and KAR14), which have detrital zircon age populations very similar to those seen in Palaeozoic and Mesozoic siliciclastic sediments of the central North Gondwana margin (e.g. Meinhold et al. 2011, 2013; Dörr et al. 2015). Future studies may shed light on their palaeotectonic history. Moreover, Devonian-aged zircon populations characterise some of the Late Triassic Karakaya Complex sandstones exposed in the Sakarya Zone of NW Turkey (Ustaömer et al. 2016). Some of the studied Karaburun sediments (e.g. Dikendağı and Gerence formations) also have zircon grains with such ages. Based on their zircon age populations (with the exception of the occurrence of Late Triassic zircons ages), some of the Karaburun sediments share similarities with the Karakaya Complex sandstones of the Sakarya Zone.

Conclusions

Our study provides the first comprehensive U–Pb database of Palaeozoic and Mesozoic siliciclastic sedimentary rocks from the Karaburun Peninsula of western Turkey. These data give new constraints for the timing of sediment deposition and stratigraphy of the study area as well as information on provenance. The most important findings of this study are as followed:

- Küçükbahçe and Dikendağı formations are not of Ordovician or Early Carboniferous age: sediment accumulation probably began in mid-Carboniferous times and continued to at least Pennsylvanian–Cisuralian.
- Zircons from the Küçükbahçe Formation yielded consistent and homogenous results throughout all samples. In contrast, the Dikendağı Formation is characterised by large heterogeneity.
- The Alandere Formation (Serpukhovian–Bashkirian) is the oldest formation of Karaburun Peninsula.
- The Palaeozoic sequence composed of the Küçükbahçe, Dikendağı and Alandere formations is, in fact, a stack of units formed by supposed post-Cretaceous thrusting.
- Karaburun, Chios and Inousses sediments are closely related and share similar provenance. They were located along the southern margin of Eurasia during Late Palaeozoic time, the exception being two samples from the Dikendağı Formation.
- Some of the Late Palaeozoic and Triassic sediments of Karaburun Peninsula share similarities in respect of detrital zircon ages with the Karakaya Complex sandstones of the Sakarya Zone in NW Turkey.

Acknowledgements

We gratefully acknowledge financial support by the German Research Foundation (DFG grant ME 3882/3-1) and the Göttingen University start-up funding for young academics. We thank Wolfgang Dörr and Paraskevas Xypolias for constructive reviews and Axel Gerdes for his editorial handling of the manuscript.

References

Abbo A, Avigad D, Gerdes A, Güngör T (2015) Cadomian basement and Paleozoic to Triassic siliciclastics of the Taurides (Karacahisar dome, south-central Turkey): Paleogeographic constraints from U–Pb–Hf in zircons. Lithos 227:122–139

Akal C, Koralay O, Candan O, Oberhänsli R, Chen F (2011) Geodynamic significance of the Early Triassic Karaburun granitoid (Western Turkey) for the opening history of Neo-Tethys. Turkish J Earth Sci 2011:255–271

Allen CM, Barnes CG (2006) Ages and some cryptic sources of Mesozoic plutonic rocks in the Klamath Mountains, California and Oregon. In: Snoke AW, Barnes CG (eds) Geological Studies in the Klamath Mountains Province, California and Oregon: A volume in honor of William P. Irwin. Geol Soc Am Spec Pap 410:223–245

Anders B, Reischmann T, Kostopoulos D (2007) Zircon geochronology of basement rocks from the Pelagonian Zone, Greece: constraints on the pre-Alpine evolution of the westernmost Internal Hellenides. Int J Earth Sci 96:639–661

Aysal N, Ustaömer T, Öngen S, Keskin M, Köksal S, Peytcheva I, Fanning M (2012) Origin of the Early-Middle Devonian magmatism in the Sakarya Zone, NW Turkey: Geochronology, geochemistry and isotope systematics. J Asian Earth Sci 45:201–222

Besenecker H, Dürr S, Herget G, Jacobshagen V, Kauffmann GL, Lüdtke G, Roth W, Tietze KW (1968) Geologie von Chios (Ägäis). Geol Palaeontol 2:121–150

Besenecker H, Dürr S, Herget G, Kauffmann G, Lüdtke G, Roth W, Tietze KW (1971) Geological Map of Greece, Chios sheet, 1:50 000 (two sheets: Northern and Southern) Institute for Geology and Subsurface Research, Athens

Brinkmann R, Flügel E, Jacobshagen V, Lechner H, Rendel B, Trick P (1972) Trias, Jura und Unterkreide der Halbinsel Karaburun (West Anatolien). Geol Palaeontol 6:139–150

Bröcker M, Pidgeon RT (2007) Protolith ages of meta-igneous and metatuffaceous rocks from the Cycladic Blueschist Unit, Greece: results of a reconnaissance U-Pb zircon study. J Geol 115:83–98

Çakmakoğlu A, Bilgin Z (2006) Pre-Neogene stratigraphy of the Karaburun Peninsula (W of İzmir Turkey). Miner Res Exp 132:33–61

Carrigan CW, Mukasa SB, Haydoutov I, Kolcheva K (2005) Age of Variscan magmatism from the Balkan sector of the orogen, central Bulgaria. Lithos 82:125–147

Chatzaras V, Dörr W, Gerdes A, Krahl J, Xypolias P, Zulauf G (2016) Tracking the late Paleozoic to early Mesozoic margin of northern Gondwana in the Hellenides: paleotectonic constraints from U–Pb detrital zircon ages. Int J Earth Sci. doi: 10.1007/s00531-016-1298-z

Chen F, Siebel W, Satir M, Terzioğlu M, Saka K (2002) Geochronology of the Karadere basement (NW Turkey) and implications for the geological evolution of the İstanbul zone. Int J Earth Sci 91:469–481

Dörr W, Zulauf G, Gerdes A, Lahaye Y, Kowalczyk G (2015) A hidden Tonian basement in the eastern Mediterranean: Age constraints from U–Pb data of magmatic and detrital zircons of the External Hellenides (Crete and Peloponnesus). Precambrian Res 258:83–108

Engel M, Reischmann T (1998) Single zircon geochronology of orthogneisses from Paros, Greece. Bull Geol Soc Greece 32:91–99

Ercan T, Türkecan A, Satır M (2000) Karaburun Yaramadasının Neojen volkanizması [Neogene volcanism of Karaburun Peninsula]. Cumhuriyetin 75. Yıldönümü Yerbilimleri ve Madencilik Kongresi Bildiriler Kitabı, Min Res Explor Inst Turkey Ankara, pp 1–18

Erdoğan B, Altıner D, Güngör T, Özer S (1990) Stratigraphy of Karaburun peninsula. Bull Miner Res Explor Inst Turkey 111:1–23

Erdoğan B, Güngör T, Özer S (2000) Stratigraphy of Karaburun Peninsula Excursion Guide, Int Earth Sci Colloq Aegean Region (IESCA) 2000, İzmir, pp 1–32

Erkül ST, Sözbilir H, Erkül F, Helvacı C, Ersoy EY, Sümer Ö (2008) Geochemistry of I-type granitoids in the Karaburun Peninsula, West Turkey: Evidence for Triassic continental arc magmatism following closure of the Palaeotethys. Isl Arc 17:394–418

Fedo CM, Sircombe KN, Rainbird RH (2003) Detrital zircon analysis of the sedimentary record. In: Hanchar JM, Hoskin PO (eds) Zircon, vol 53. Rev Mineral Geochem, pp 277-303

Gehrels GE, Valencia VA, Ruiz J (2008) Enhanced precision, accuracy, efficiency, and spatial resolution of U-Pb ages by laser ablation-multicollector-inductively coupled plasma-mass spectrometry. Geochem Geophy Geosys 9(3), Q03017. doi:10.1029/2007GC001805

Gessner K, Collins AS, Ring U, Güngör T (2004) Structural and thermal history of poly-orogenic basement: U-Pb geochronology of granitoid rocks in the southern Menderes Massif, Western Turkey. J Geol Soc London 161:93–101

Gradstein FM, Ogg G, Schmitz M (2012) The Geologic Time Scale, 2-Volume Set. Elsevier, Amsterdam, 1176 pp

Graf J (2001) Alpine tectonics in western Bulgaria: Cretaceous compression of the Kraište region and Cenozoic exhumation of the crystalline Osogovo-Lisec Complex. Ph.D. thesis, ETH Zürich, Switzerland, 182 pp

Hetzel R, Reischmann T (1996) Intrusion age of Pan-African augen gneisses in the southern Menderes Massif and the age of cooling after Alpine ductile extensional deformation. Geol Mag 133:565–572

Hetzel R, Romer RL, Candan O, Passchier CW (1998) Geology of the Bozdag area, central Menderes massif, SW Turkey: Pan-African basement and Alpine deformation. Geol Rundsch 87:394–406

Himmerkus F, Reischmann T, Kostopoulos D (2006) Late Proterozoic and Silurian basement units within the Serbo-Macedonian Massif, northern Greece: the significance of terrane accretion in the Hellenides. In: Robertson AHF, Mountrakis D (eds) Tectonic development of the Eastern Mediterranean Region, vol 260. Geol Soc Lond Spec Publ, pp 35–50

Himmerkus F, Reischmann T, Kostopoulos D (2007) Gondwana-derived terranes in the northern Hellenides. In: Hatcher RD, Carlson MP, McBride JH, Martínez Catalán JR (eds) 4-D Framework of continental crust, vol 200. Geol Soc Am Mem, pp 379-39

Himmerkus F, Reischmann T, Kostopoulos D (2009a) Serbo-Macedonian revisited: A Silurian basement terrane from northern Gondwana in the Internal Hellenides, Greece. Tectonophysics 473:20–35

Himmerkus F, Reischmann T, Kostopoulos D (2009b) Triassic rift-related meta-granites in the Internal Hellenides, Greece. Geol Mag 146:252–265

Jacobshagen V (1986) Geologie von Griechenland. Gebrüder Borntraeger, Berlin, pp 1–363

Kalafatçıoğlu (1961) A geological study in the Karaburun Peninsula. Bull Miner Res Explor Inst Turkey 56:40–49

Kalvoda J (2003) Carboniferous foraminiferal paleobiogeography in Turkey and its implications for plate tectonic reconstructions. Riv Ital Paleont Strat 109:255–266

Kauffmann G (1965) Fossil-belegtes Altpaläozoikum im Nordost-Teil der Insel Chios (Ägäis). N Jb Geol Paläont Monatshefte 1965:647–659

Keay S, Lister G, Buick I (2001) The timing of partial melting, Barrovian metamorphism and granite intrusion in the Naxos metamorphic core complex, Cyclades, Aegean Sea, Greece. Tectonophysics 342:275–312

Kilias A (1987) Die Phyllit–Schiefer-Serie der Insel Oinousai: Mikrostrukturen, Kinematik und tektonische Stellung im Helleniden Orogen (Griechenland). Geol Balc 17:83–90

Kooijman E, Berndt J, Mezger K (2012) U-Pb dating of zircon by laser ablation ICP-MS: recent improvements and new insights. Eur J Mineral 24:5–21

Koralay OE, Satir M, Dora OÖ (2001) Geochemical and geochronological evidence for Early Triassic calc-alkaline magmatism in the Menderes Massif, western Turkey. Int J Earth Sci 89:822–835

Kounov A (2002) Thermotectonic evolution of Kraishte, western Bulgaria. Ph.D. thesis, ETH Zürich, Switzerland, 219 pp

Kozur H (1995) New stratigraphic results on the Palaeozoic of the Western parts of the Karaburun Peninsula, Western Turkey. In: Pişkin O, Ergün M, Savaşçin MY, Tarcan G (eds) Proceedings of International Earth Sciences Colloquium on the Aegean Region, İzmir, pp 289–308

Kozur H (1997) First discovery of Muellerisphaerida (inc. sedis) and *Eoalbaillella* (Radiolaria) in Turkey and the age of the siliciclastic sequence (clastic series) in Karaburun peninsula. Freib Forschungshefte C, Geowissenschaften Geol C 46:33–59

Kozur H (1998) The age of the siliciclastic series (“Karareis Formation”) of the western Karaburun peninsula, western Turkey. In: Szaniawski H (ed) Proceedings of the Sixth European Conodont Symposium (ECOS VI), vol 58. Palaeontologia Polonica, pp 171–

189pp 171–189

Kröner A, Şengör AMC (1990) Archean and Proterozoic ancestry in late Precambrian to early Paleozoic crustal elements of southern Turkey as revealed by single-zircon dating. Geology 18:1186–1190

Loos S, Reischmann T (1999) The evolution of the southern Menderes Massif in SW Turkey as revealed by zircon dating. J Geol Soc London 156:1021–1030

Ludwig K (2003) Isoplot/Ex 3.00. A Geochronological Toolkit for Microsoft Excel. Berkeley Geochron Cent Spec Publ 4:1–70

Marsellos AE, Foster DA, Kamenov GD, Kyriakopoulos K (2012) Detrital zircon U-Pb data from the Hellenic south Aegean belts: constraints on the age and source of the South Aegean basement. J Virt Explor. doi:10.3809/jvirtex.2011.00284

Meinhold G, Kostopoulos D, Reischmann T (2007) Geochemical constraints on the provenance and depositional setting of sedimentary rocks from the islands of Chios, Inousses and Psara, Aegean Sea, Greece: implications for the evolution of Palaeotethys. J Geol Soc London 164:1145–1163

Meinhold G, Frei D (2008) Detrital zircon ages from the islands of Inousses and Psara, Aegean Sea, Greece: constraints on depositional age and provenance. Geol Mag 145:886–891

Meinhold G, Morton AC, Avigad D (2013) New insights into peri-Gondwana paleogeography and the Gondwana super-fan system from detrital zircon U–Pb ages. Gondwana Res 23:661–665.

Meinhold G, Anders B, Kostopoulos D, Reischmann T (2008a) Rutile chemistry and thermometry as provenance indicator: An example from Chios Island, Greece. Sediment Geol 203:98–111

Meinhold G, Reischmann T, Kostopoulos D, Lehnert O, Matukov D, Sergeev S (2008b)

Provenance of sediments during subduction of Palaeotethys: Detrital zircon ages and olistolith analysis in Palaeozoic sediments from Chios Island, Greece. Palaeogeogr Palaeoclimatol Palaeoecol 263:71–91

Meinhold G, Kostopoulos D, Frei D, Himmerkus F, Reischmann T (2010) U–Pb LA-SF-ICP-MS zircon geochronology of the Serbo-Macedonian Massif, Greece: palaeotectonic constraints for Gondwana-derived terranes in the Eastern Mediterranean. Int J Earth Sci 99:813–832

Meinhold G, Morton AC, Fanning CM, Frei D, Howard JP, Philips RJ, Strogen D, Whitham AG (2011) Evidence from detrital zircons for recycling of Mesoproterozoic and Neoproterozoic crust recorded in Paleozoic and Mesozoic sandstones of southern Libya. Earth Planet Sci Lett 312:164–175

Moix P, Beccaletto L, Kozur HW, Hochard C, Rosselet F, Stampfli GM (2008) A new classification of the Turkish terranes and sutures and its implication for the paleotectonic history of the region. Tectonophysics 451:7–39

Mountrakis D, Sapountzis E, Kilias A, Eleftheriadis G, Christofides G (1983) Paleogeographic conditions in the western Pelagonian margin in Greece during the initial rifting of the continental area. Can J Earth Sci 20:1673–1681

Nance RD, Murphy JB (1994) Contrasting basement isotopic signatures and the palinspastic restoration of peripheral orogens: Example from the Neoproterozoic Avalonian-Cadomian belt. Geology 22:617–620

Okay AI, Tüysüz O (1999) Tethyan sutures of northern Turkey. In: Durand B, Jolivet L, Horivath F, Séranne M (eds) The Mediterranean Basin: Tertiary extension within the Alpine Orogen, vol 156. Geol Soc Lond Spec Publ, pp 475–515

Okay AI, Satir M, Maluski M, Siyako M, Monie P, Metzger R, Akyüz S (1996) Palaeo- and Neo-Tethyan events in northwestern Turkey: geologic and geochronologic constraints. In: Yin A, Harrison TM (eds) The tectonic evolution of Asia. Cambridge Universty Press, pp 420–441

Okay AI, Satir M, Siebel W (2006) Pre-Alpide Palaeozoic and Mesozoic orogenic events in the Eastern Mediterranean region. In: Gee DG, Stephenson RA (eds) European Lithosphere Dynamics, vol 32. Geol Soc Lond Mem, pp 389–405

Okay AI, Satır M, Shang CK (2008) Ordovician metagranitoid from the Anatolide-Tauride Block, northwest Turkey: geodynamic implications. Terra Nova 20:280–288

Özbey Z, Ustaömer T, Robertson AHF, Ustaömer PA (2013) Tectonic significance of Late Ordovician granitic magmatism and clastic sedimentation on the northern margin of Gondwana (Tavsanli Zone, NW Turkey). J Geol Soc London 170:159–173

Özmen F, Reischmann T (1999) The age of the Sakarya continent in W Anatolia: implications for the evolution of the Aegean region. J Conf Abstr 4:805

Pe-Piper G, Piper DJW (2002) The igneous rocks of Greece: the anatomy of an orogen Gebrüder Borntraeger, Stuttgart, 573 pp

Peytcheva I, von Quadt A (2004) The Palaeozoic protoliths of the Central Srednogorie, Bulgaria: records in zircons from basement rocks and Cretaceous magmatites. 5th ISEMG Conf Proc 1:392–395

Philippson A (1911) Reisen und Forschungen im westlichen Kleinasien, 2. Heft: Ionien und das westliche Lydien. Peterm Mitt Erg H 172, 1–100

Reischmann T (1998) Pre-alpine origin of tectonic units from the metamorphic complex of Naxos, Greece, identified by single Pb/Pb dating. Bull Geol Soc Greece 32:101–111

Robertson AHF, Pickett EA (2000) Palaeozoic–Early Tertiary Tethyan evolution of mélanges, rift and passive margin units in the Karaburun Peninsula (western Turkey) and Chios Island (Greece). In: Bozkurt E, Winchester JA, Piper JDA (eds) Tectonic and magmatism in Turkey and the surrounding area, vol 173. Geol Soc Lond Spec Publ, pp 43–82

Robertson AHF, Ustaömer T, Pickett EA, Collins AS, Andrew T, Dixon JE (2004) Testing models of Late Palaeozoic–Early Mesozoic orogeny in Western Turkey: support for an evolving open-Tethys model. J Geol Soc London 161:501–511

Robertson AHF, Ustaömer T (2009) Upper Palaeozoic subduction/accretion processes in the closure of Palaeotethys: Evidence from the Chios Melange (E Greece), the Karaburun Melange (W Turkey) and the Teke Dere Unit (SW Turkey). Sediment Geol 220:29–59

Rosselet F, Stampfli G (2003) The Paleozoic siliclastic sequences in Karaburun, a remnant of the Paleotethys fore-arc basin in Western Turkey. Geophys Res Abstr 5:09770

Şengör AMC, Yilmaz Y, Sungurlu O (1984) Tectonics of the Mediterranean Cimmerides: nature and evolution of the western termination of Palaeo-Tethys. In: Dixon JE, Robertson AHF (eds) The geological evolution of the eastern Mediterranean, vol 17. Geol Soc Lond Spec Publ, pp 77–112

Spencer CJ, Prave AR, Cawood PA, Roberts NMW (2014) Detrital zircon geochronology of the Grenville/Llano foreland and basal Sauk Sequence in west Texas, USA. Geol Soc Am Bull 126:1117–1128

Stampfli GM (2000) Tethyan oceans. In: Bozkurt E, Winchester JA, Piper JDA (eds) Tectonics and magmatism in Turkey and the surrounding area, vol 173. Geol Soc Lond Spec Publ, pp 1–23

Stampfli GM, Borel G. (2002) A plate tectonic model for the Paleozoic and Mesozoic constrained by dynamic plate boundaries and restored synthetic oceanic isochrons. Earth Planet Sci Lett 196:17–33

Stampfli GM, Vavassis I, De Bono A, Rosselet F, Matti B, Bellini M (2003) Remnants of the Paleotethys oceanic suture-zone in the western Tethyn area. In: Cassinis G (ed) Stratigraphic and Structural Evolution on the Late Carboniferous to Triassic Continental and

Marine Successions in Tuscany (Italy): Regional Reports and General Correlation, vol speciale 2. Boll Soc Geol Ital, pp 1–23

Sunal G (2012) Devonian magmatism in the western Sakarya Zone, Karacabey region, NW Turkey. Geodin Acta 25:183–201

Titorenkova R, Macheva L, Zidarov N, von Quadt A, Peytcheva I (2003) Metagranites from SW Bulgaria as a part of the Neoproterozoic to early Paleozoic system in Europe: new insight from zircon typology, U-Pb isotope data and Hf-tracing. Geophys Res Abstr 5:08963

Tomaschek F, Kennedy A, Keay S, Ballhaus C (2001) Geochronological constraints on Carboniferous and Triassic magmatism in the Cyclades: SHRIMP U–Pb ages of zircons from Syros, Greece. J Conf Abstr 6:315

Turpaud P, Reischmann T (2010) Characterisation of igneous terranes by zircon dating: implications for UHP occurrences and suture identification in the Central Rhodope, northern Greece. Int J Earth Sci 99:567–591

Ustaömer PA, Mundil R, Renne PR (2005) U/Pb and Pb/Pb zircon ages for arc-related intrusions of the Bolu Massif (W Pontides, NW Turkey): evidence for Late Precambrian (Cadomian) age. Terra Nova 17:215–223

Ustaömer PA, Ustaömer T, Robertson AHF (2012) Ion probe U–Pb dating of the central Sakarya basement: a peri-Gondwana terrane intruded by Late Lower Carboniferous subduction/collision-related granitic rocks. Turkish J Earth Sci 21:905–932

Ustaömer T, Ustaömer PA, Robertson AHF, Gerdes A (2016) Implications of U–Pb and Lu–Hf isotopic analysis of detrital zircons for the depositional age, provenance and tectonic setting of the Permian–Triassic Palaeotethyan Karakaya Complex, NW Turkey. Int J Earth Sci 105:7–38

Vermeesch P (2012) On the visualisation of detrital age distributions. Chem Geol 312–313:190–

194

von Quadt A, Graf J, Bernoulli D (2000) Pre-Variscan and Tertiary magmatism in western Bulgaria (Kraiste) based on U–Pb single zircon analyses, trace and REE element distribution and Sm/Nd – Rb/Sr investigation. Terra Nostra 2000/1:87

Wiedenbeck M, Allé P, Corfu F, Griffin WL, Meier M, Oberli F, von Quadt A, Roddick JC, Spiegel W (1995) Three natural zircon standards for U–Th–Pb, Lu–Hf, trace element and REE analyses. Geostand Newslett 19:1–23

Windley BF (1995) The evolving continents, 3rd edition Wiley, Chichester, 544 pp

Xypolias P, Dörr W, Zulauf G (2006) Late Carboniferous plutonism within the pre-Alpine basement of the External Hellenides (Kithira, Greece): evidence from U-Pb zircon dating. J Geol Soc London 163:539–547

Xypolias P, Koukouvelas I, Zulauf G (2008) Cenozoic tectonic evolution of northeastern Apulia: insights from a key study area in the Hellenides (Kythira, Greece). Z dt 159:439–455

Zanchi A, Garzanti E, Larghi C, Angiolini L, Gaetani M (2003) The Variscan orogeny in Chios (Greece): Carboniferous accretion along a Palaeotethyan active margin. Terra Nova 15:213–223

Zlatkin O, Avigad D, Gerdes A (2013) Evolution and provenance of Neoproterozoic basement and Lower Paleozoic siliciclastic cover of the Menderes Massif (western Taurides): Coupled U–Pb–Hf zircon isotope geochemistry. Gondwana Res 23:682–700

Zulauf G, Dörr W, Fisher-Spurlock SC, Gerdes A, Chatzaras V, Xypolias P (2015) Closure of the Paleotethys in the External Hellenides: Constraints from U–Pb ages of magmatic and detrital zircons (Crete). Gondwana Res 28:642–667

Zulauf G, Dörr W, Krahl J, Lahaye Y, Chatzaras V, Xypolias P (2016) U–Pb zircon and biostratigraphic data of high-pressure/low-temperature metamorphic rocks of the Talea Ori:

tracking the Paleotethys suture in central Crete, Greece. Int J Earth Sci. doi:10.1007/s00531-016-1307-2

FIGURE CAPTIONS

Fig. 1 Simplified geotectonic map of the Eastern Mediterranean region (after Jacobshagen 1986; Okay and Tüysüz 1999; Okay et al. 2006)

Fig. 2 Simplified geological map of the study area with sample locations. The Karaburun map is modified after Çakmakoğlu and Bilgin (2006) and the Chios and Inousses maps are modified after Meinhold et al. (2007). The sedimentary succession of Inousses Island is correlated with the Küçükbahçe Formation of Karaburun Peninsula, based on field observations and data of this study

Fig. 3 Stratigraphic sections of Chios and Karaburun. For simplification, the ?Late Permian Tekedağı Formation, consisting of bioclastic limestone, dolomitic limestone, partly oolitic/pisolitic, and limestone with sandstone, siltstone and marl interfingers (Çakmakoğlu and Bilgin 2006), is not shown here. The Tekedağı Formation is only present in a small area to the NW of Gerence Bay. This formation probably correlates with the stratigraphically younger part of the Permian limestones from the Upper Unit of Chios Island. Biostratigraphic data from Brinkmann et al. (1972), Çakmakoğlu and Bilgin (2006), Erdoğan et al. (1990, 2000), Kozur (1997, 1998). Blocks / olistoliths in the Palaeozoic succession of Karaburun Peninsula have been described by Kozur (1998) and Robertson and Ustaömer (2009)

Fig. 4 Field photographs from the Karaburun Peninsula. **a** View to the Mesozoic platform carbonates of the Camiboğazı Formation. **b** Outcrop of conglomerates from the basal part of the Gerence Formation (North of Gerence Bay). **c–d** Low-grade metamorphosed mudrocks of the Küçükbahçe Formation (NW part of Karaburun Peninsula) (pen for scale: 15 cm; hammer for scale: 30 cm). **e** Section from silt-/sandstone succession of the Dikendağı Formation (North of Gerence Bay). **f** Chevron folds in black chert in the Dikendağı Formation (North of Gerence Bay). In **c–f** hammer (30 cm long) and pen (15 cm long) for scale, respectively

Fig. 5 U–Pb concordia plots showing LA-ICP-MS data of samples from the Triassic successions. Data point error ellipses indicate 2σ uncertainties. Shaded grey ellipses outline areas that are shown as close-up

Fig. 6 Histograms and kernel density estimates of detrital U–Pb zircon ages from the Triassic successions

Fig. 7 U–Pb concordia plots showing LA-ICP-MS data of samples from the Küçükbahçe Formation. Data point error ellipses indicate 2σ uncertainties. Shaded grey ellipses outline areas that are shown as close-up

Fig. 8 Histograms and kernel density estimates of detrital U–Pb zircon ages from the Küçükbahçe Formation

Fig. 9 U–Pb concordia plots showing LA-ICP-MS data of samples from the Dikendağı and Alandere formations. Data point error ellipses indicate 2σ uncertainties. Shaded grey ellipses outline areas that are shown as close-up

Fig. 10 Histograms and kernel density estimates of detrital zircon U–Pb ages from the Dikendağı and Alandere formations

Fig. 11 Percentages of detrital zircon U–Pb ages for studied samples

Fig. 12 Histograms and kernel density estimates of detrital zircon U–Pb ages from the Küçükbahçe Formation of Karaburun Peninsula (*n* = 267, this study) and Inousses Island (*n* = 49, Meinhold and Frei 2008) for comparison

Fig. 13 Revised stratigraphic section of Karaburun Peninsula. Sediment accumulation of the Küçükbahçe and Dikendağı formations most probably began in the mid-Carboniferous and continued to at least Pennsylvanian–Cisuralian. The Alandere Formation represents the oldest part of the mélange. Contacts between the Alandere, Dikendağı and Küçükbahçe formations are supposed to be rather tectonic than gradational. Blocks / olistoliths in the Palaeozoic succession of Karaburun Peninsula have been described by Kozur (1998) and Robertson and Ustaömer (2009)

Fig. 14 Compilation of Late Neoproterozoic and Palaeozoic zircon age distribution data of potential igneous source rocks from Greece and the surrounding region after Meinhold et al. (2008b, and reference therein), with additional data from Okay et al. (2008), Himmerkus et al. (2009a), Aysal et al. (2012), Sunal (2012), Ustaömer et al. (2012), Özbey et al. (2013), Dörr et al. (2015), Zulauf et al. (2015). For better visualisation, the dark grey fillings in the map lower right mark localities with Early to earliest Late Carboniferous ages (≥315–330 Ma) reported. Triassic igneous rocks are widespread in the Serbo-Macedonian Massif, the Pelagonian Zone, the Cycladic islands and the Menderes Massif (e.g. Tomaschek et al. 2001; Koralay et al. 2001; Bröcker and Pidgeon 2007; Anders et al. 2007; Himmerkus et al. 2009b) and for simplification are not shown in the maps. *ATB* Anatolide–Tauride Block, *EH* External Hellenides, *IZ* İstanbul Zone, *KM* Kırşehir Massif, *KR* Kraište, *MM* Menderes Massif, *MO* Moesia, *PZ* Pelagonian Zone, *RM* Rhodope Massif, *SG* Sredna Gora Zone, *SK* Sakarya, *SMM* Serbo-Macedonian Massif, *ST* Strandja, *VZ* Vardar Zone

Fig. 15 Palaeotectonic reconstruction for the Early Triassic indicating the presumed position of the Chios–Karaburun units at the southern margin of Eurasia. The exception being some rocks of the heterogeneous Dikendağı Formation, which have similar detrital zircon age populations as sediments from the northern margin of Gondwana. Base map adapted from ©Ron Blakey, Colorado Plateau Geosystems, Arizona, USA (http://cpgeosystems.com/), used with permission. *CK* Chios–Karaburun units, *Is* İstanbul Zone, *HI* Internal Hellenides, *Md* Moldanubian Zone, *Sk* Sakarya Zone, *Ta* Taurides

TABLE

Table 1 Sample list with GPS coordinates and comparison of stratigraphic ages from fossils and depositional ages derived from detrital zircon. See text for references

Electronic supplementary material

- Table S1. Detrital zircon U–Pb isotopic data

Figure1

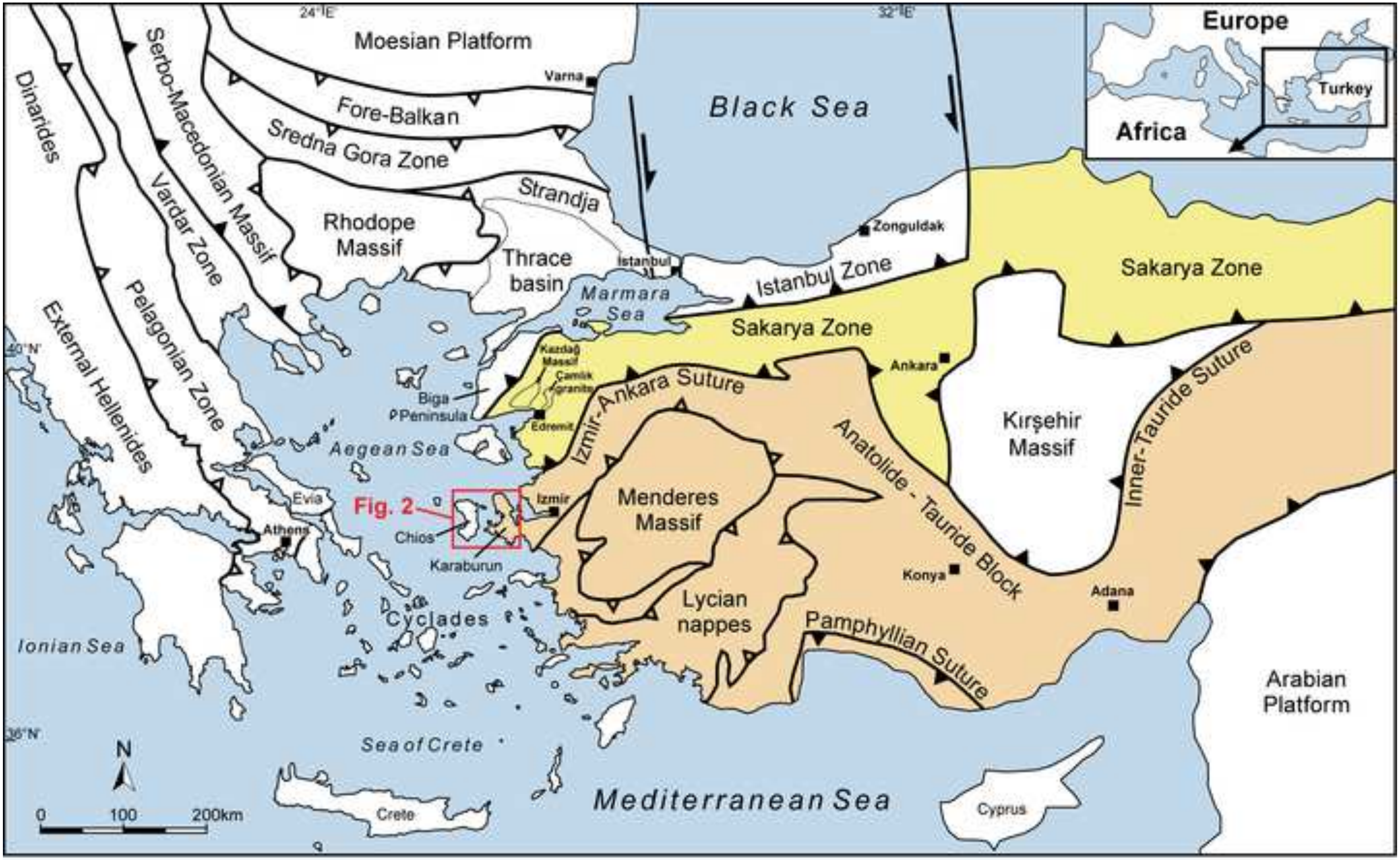

Anatolide-Tauride Block
Sakarya Zone
Suture
Thrust fault
Town

Figure2

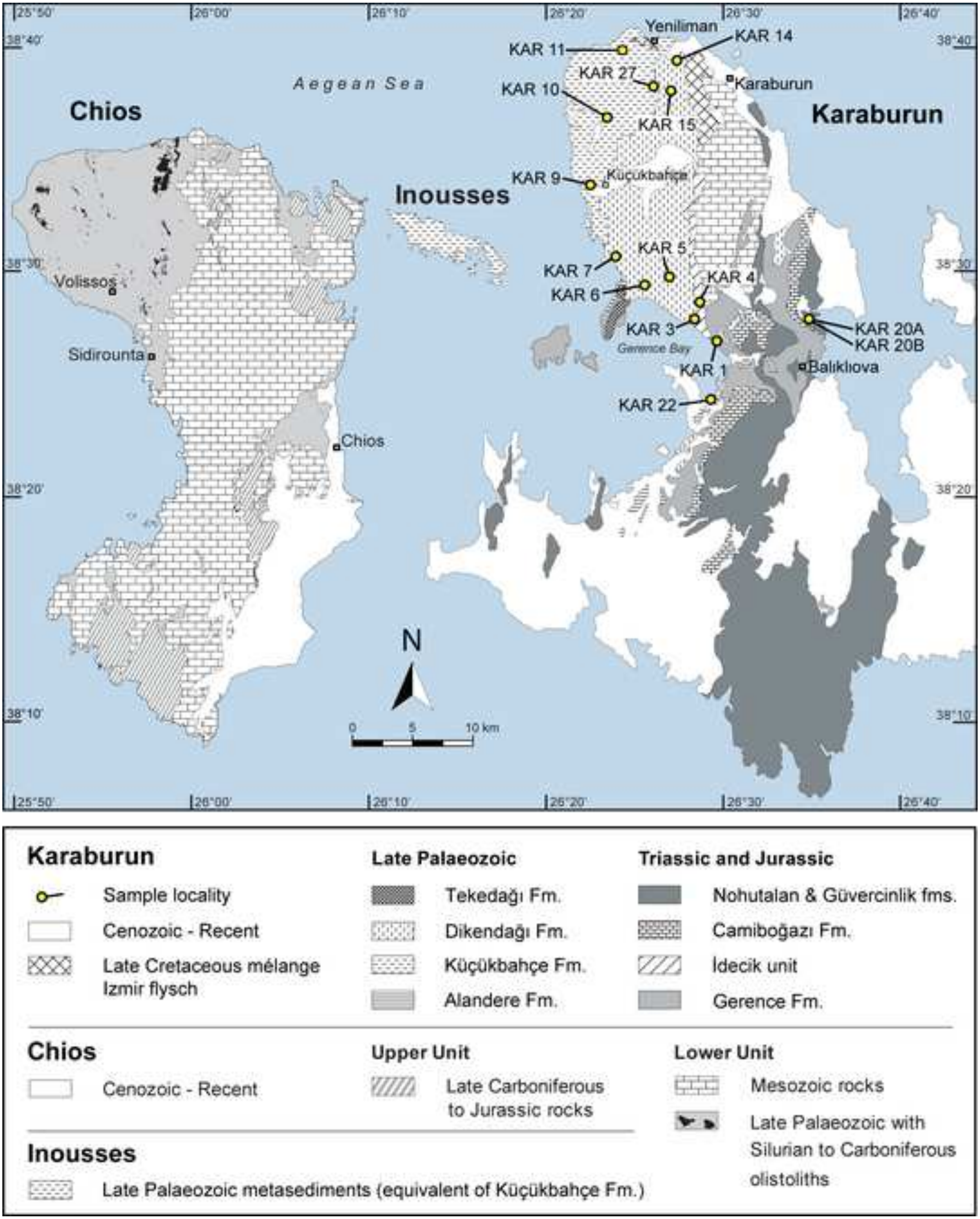

25°50'
26°00'
26°10'
26°20'
26°30'
26°40'
38°40'
38°30'
38°20'
38°10'
Aegean Sea
Chios
Inousses
Karaburun
Yeniliman
Karaburun
Küçükbahçe
Volissos
Sidirounta
Chios
Gerence Bay
Balıklıova
KAR 11
KAR 14
KAR 27
KAR 10
KAR 15
KAR 9
KAR 5
KAR 7
KAR 4
KAR 6
KAR 3
KAR 20A
KAR 20B
KAR 1
KAR 22
N
0
5
10 km
Karaburun
Sample locality
Cenozoic - Recent
Late Cretaceous mélange
Izmir flysch
Late Palaeozoic
Tekedağı Fm.
Dikendağı Fm.
Küçükbahçe Fm.
Alandere Fm.
Triassic and Jurassic
Nohutalan & Güvercinlik fms.
Camiboğazı Fm.
İdecik unit
Gerence Fm.
Chios
Cenozoic - Recent
Upper Unit
Late Carboniferous
to Jurassic rocks
Lower Unit
Mesozoic rocks
Late Palaeozoic with
Silurian to Carboniferous
olistoliths
Inousses
Late Palaeozoic metasediments (equivalent of Küçükbahçe Fm.)

Figure3

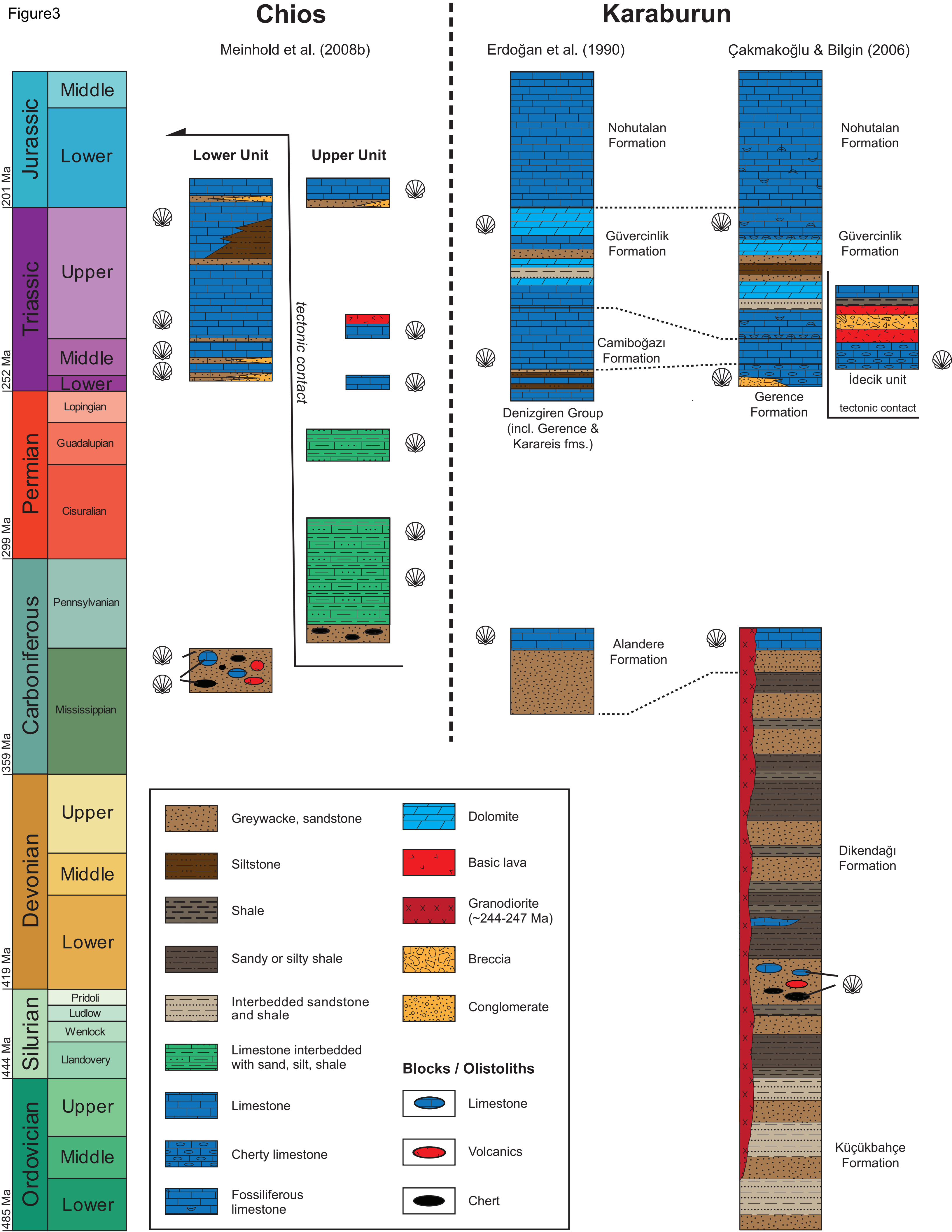

Chios
Karaburun
Meinhold et al. (2008b)
Erdoğan et al. (1990)
Çakmakoğlu & Bilgin (2006)
Jurassic
Middle
Lower
201 Ma
Triassic
Upper
Middle
Lower
252 Ma
Permian
Lopingian
Guadalupian
Cisuralian
299 Ma
Carboniferous
Pennsylvanian
Mississippian
359 Ma
Devonian
Upper
Middle
Lower
419 Ma
Silurian
Pridoli
Ludlow
Wenlock
Llandovery
444 Ma
Ordovician
Upper
Middle
Lower
485 Ma
Lower Unit
Upper Unit
tectonic contact
Nohutalan Formation
Güvercinlik Formation
Camiboğazı Formation
Denizgiren Group (incl. Gerence & Karareis fms.)
Gerence Formation
İdecik unit
tectonic contact
Alandere Formation
Dikendağı Formation
Küçükbahçe Formation
Greywacke, sandstone
Siltstone
Shale
Sandy or silty shale
Interbedded sandstone and shale
Limestone interbedded with sand, silt, shale
Limestone
Cherty limestone
Fossiliferous limestone
Dolomite
Basic lava
Granodiorite (~244-247 Ma)
Breccia
Conglomerate
Blocks / Olistoliths
Limestone
Volcanics
Chert

Figure4

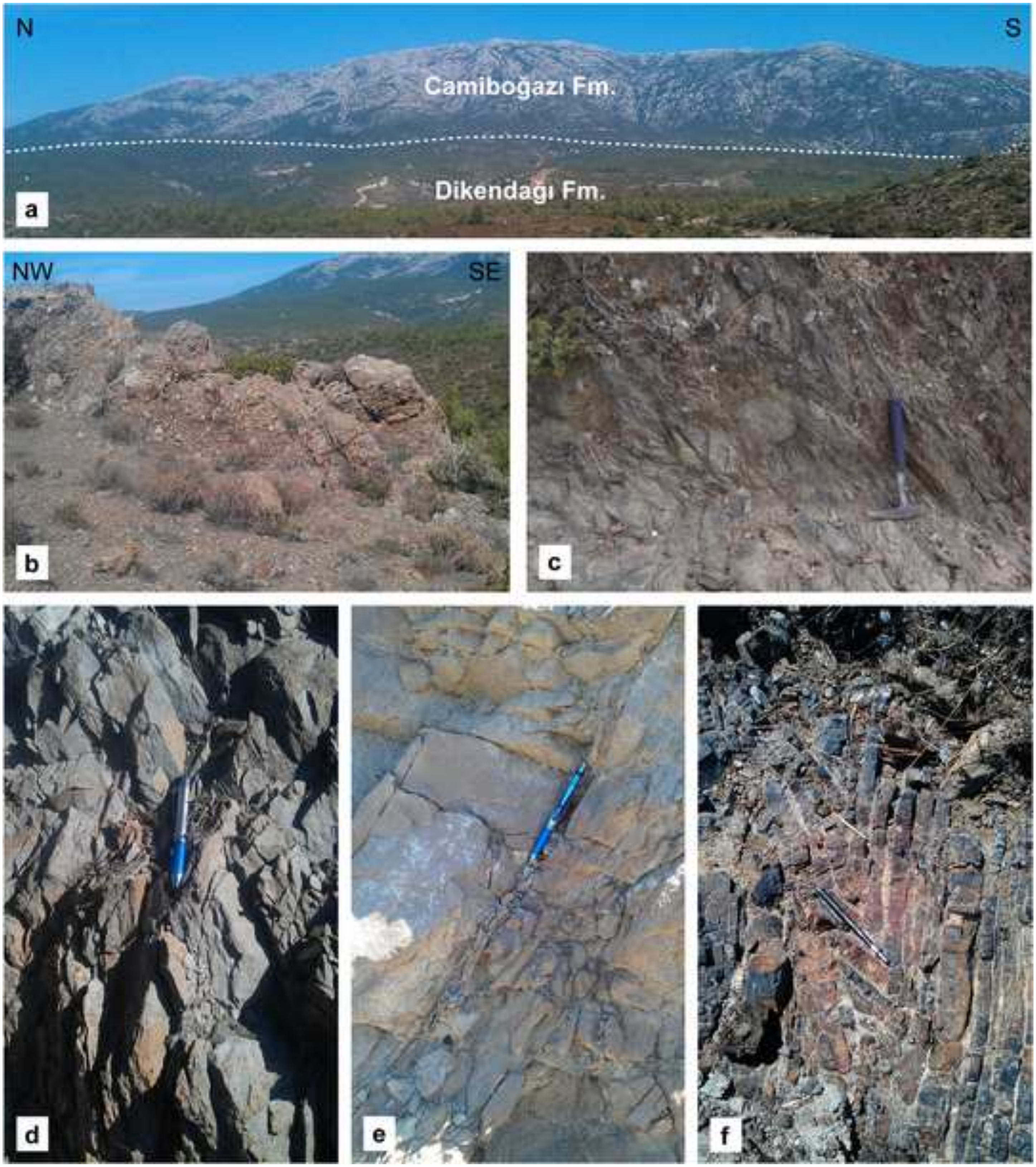

Figure5

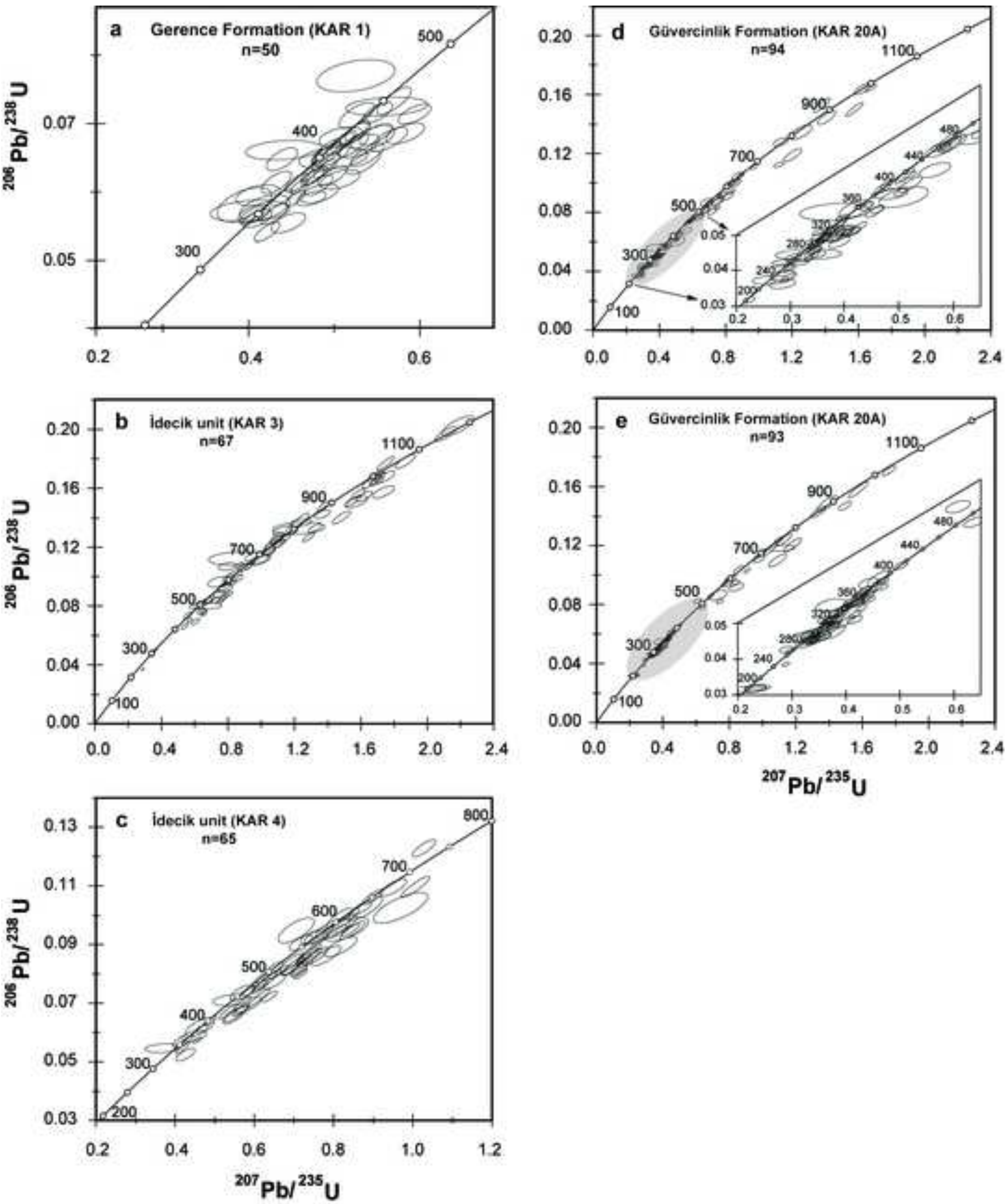

a Gerence Formation (KAR 1)
n=50
b İdecik unit (KAR 3)
n=67
c İdecik unit (KAR 4)
n=65
d Güvercinlik Formation (KAR 20A)
n=94
e Güvercinlik Formation (KAR 20A)
n=93
$^{206}Pb/^{238}U$
$^{207}Pb/^{235}U$

Figure6

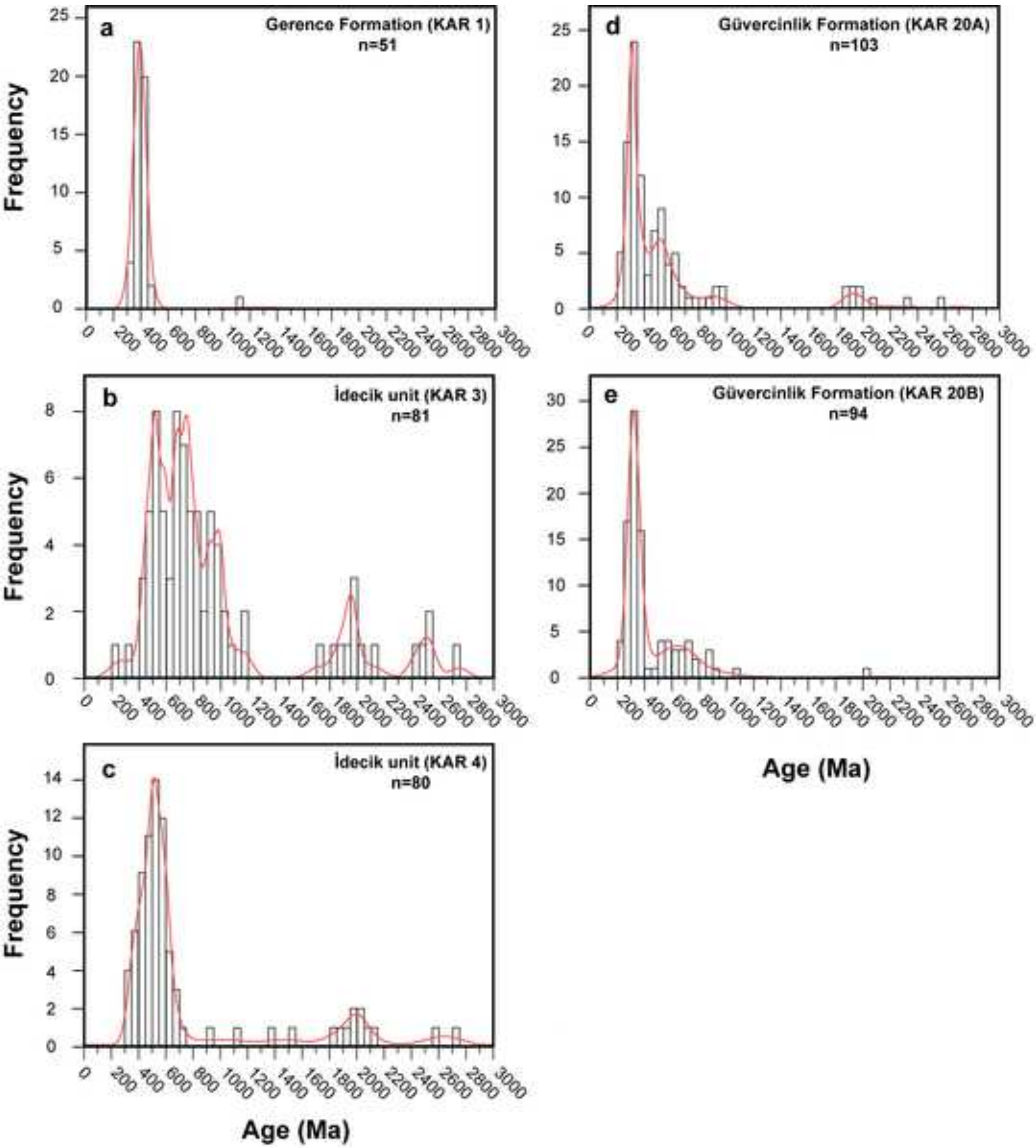

a
Gerence Formation (KAR 1)
n=51
b
İdecik unit (KAR 3)
n=81
c
İdecik unit (KAR 4)
n=80
d
Güvercinlik Formation (KAR 20A)
n=103
e
Güvercinlik Formation (KAR 20B)
n=94
Frequency
Age (Ma)

Figure7

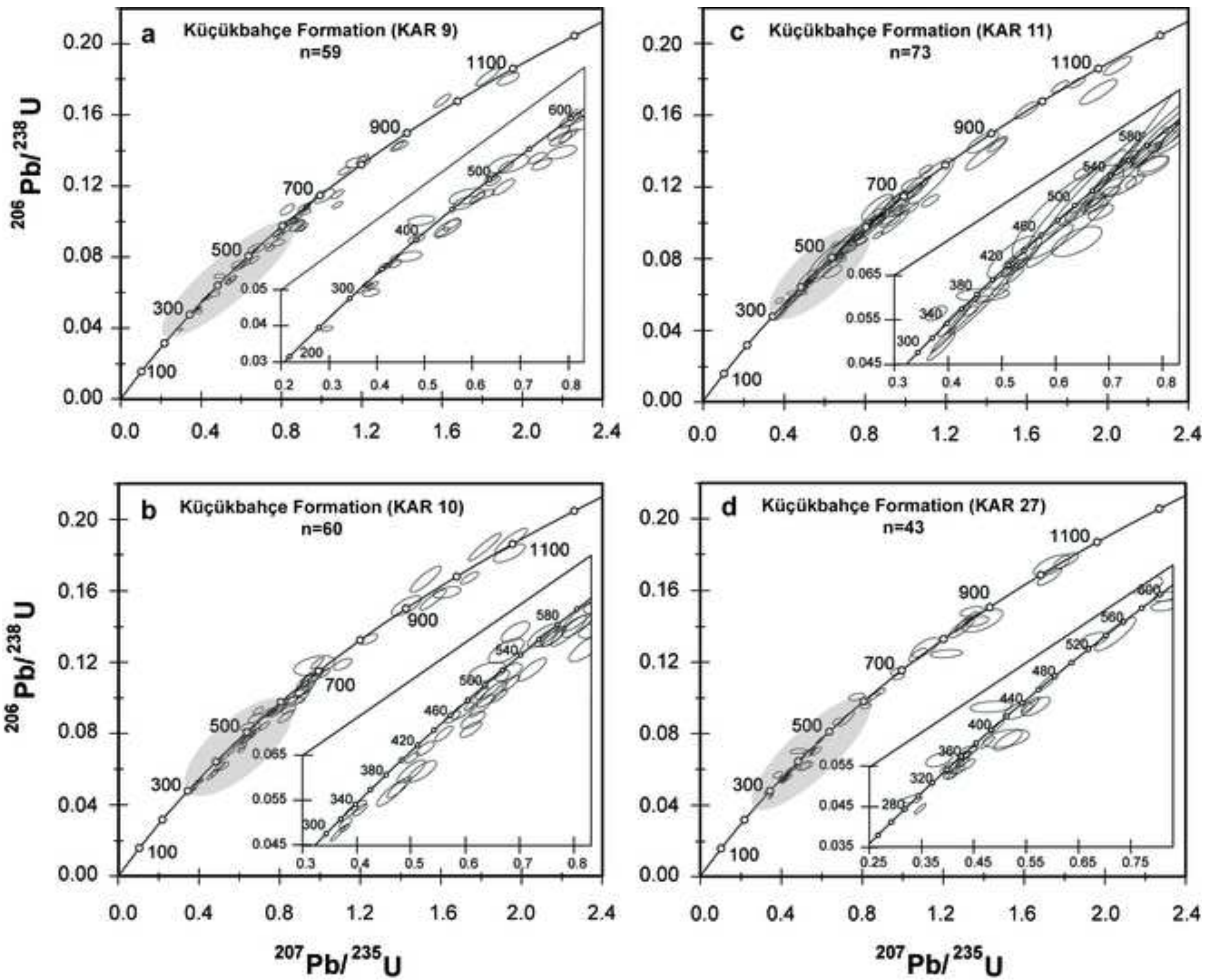

a Küçükbahçe Formation (KAR 9)
n=59
b Küçükbahçe Formation (KAR 10)
n=60
c Küçükbahçe Formation (KAR 11)
n=73
d Küçükbahçe Formation (KAR 27)
n=43
$^{206}Pb/^{238}U$
$^{207}Pb/^{235}U$

Figure8

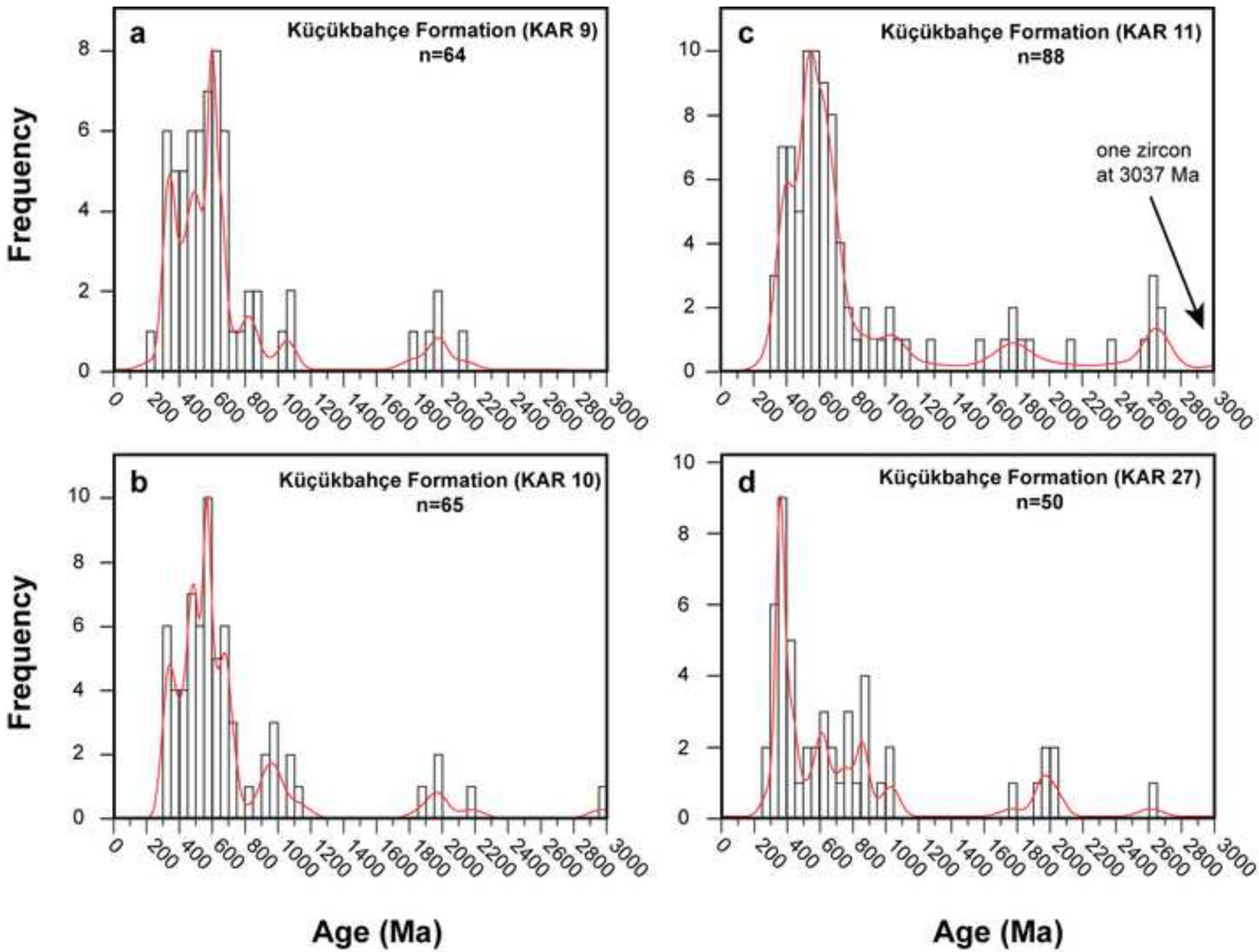

a
Küçükbahçe Formation (KAR 9)
n=64
b
Küçükbahçe Formation (KAR 10)
n=65
c
Küçükbahçe Formation (KAR 11)
n=88
one zircon
at 3037 Ma
d
Küçükbahçe Formation (KAR 27)
n=50
Frequency
Frequency
Age (Ma)
Age (Ma)
0 200 400 600 800 1000 1200 1400 1600 1800 2000 2200 2400 2600 2800 3000

Figure9

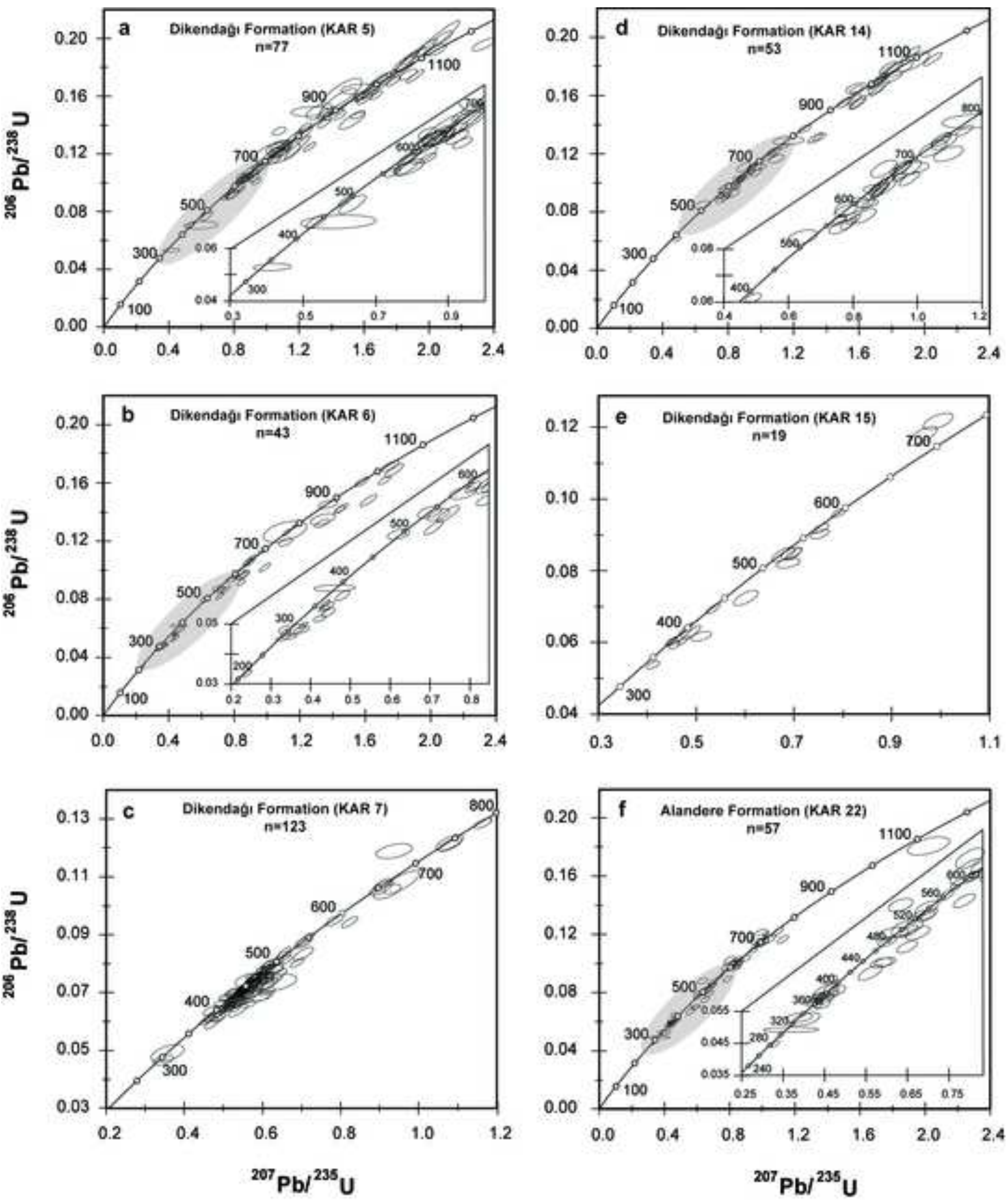
a
Dikendağı Formation (KAR 5)
n=77
d
Dikendağı Formation (KAR 14)
n=53
b
Dikendağı Formation (KAR 6)
n=43
e
Dikendağı Formation (KAR 15)
n=19
c
Dikendağı Formation (KAR 7)
n=123
f
Alandere Formation (KAR 22)
n=57
$^{206}Pb/^{238}U$
$^{207}Pb/^{235}U$

Figure10

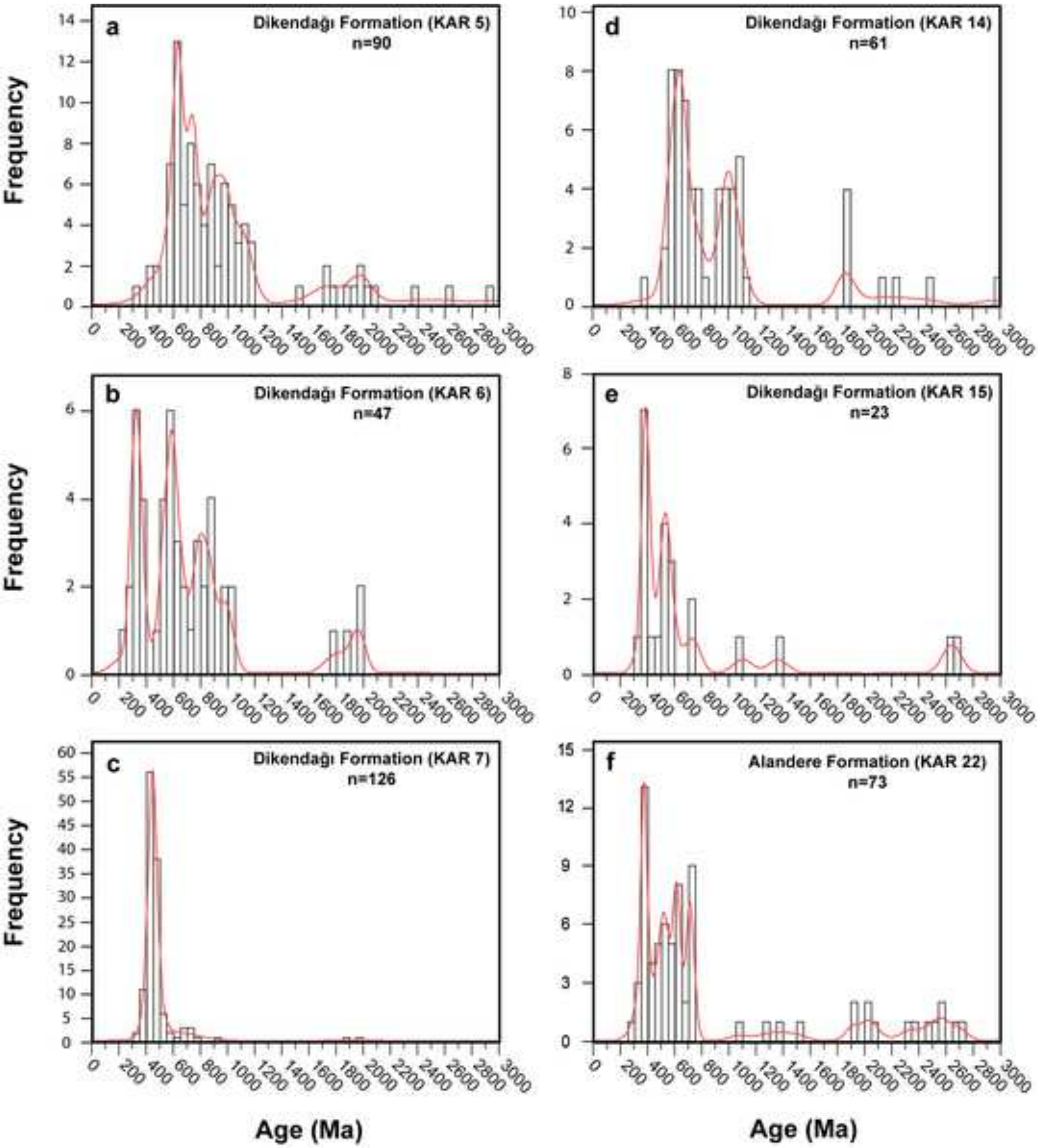

a
Dikendağı Formation (KAR 5)
n=90
b
Dikendağı Formation (KAR 6)
n=47
c
Dikendağı Formation (KAR 7)
n=126
d
Dikendağı Formation (KAR 14)
n=61
e
Dikendağı Formation (KAR 15)
n=23
f
Alandere Formation (KAR 22)
n=73
Frequency
Age (Ma)

Figure11

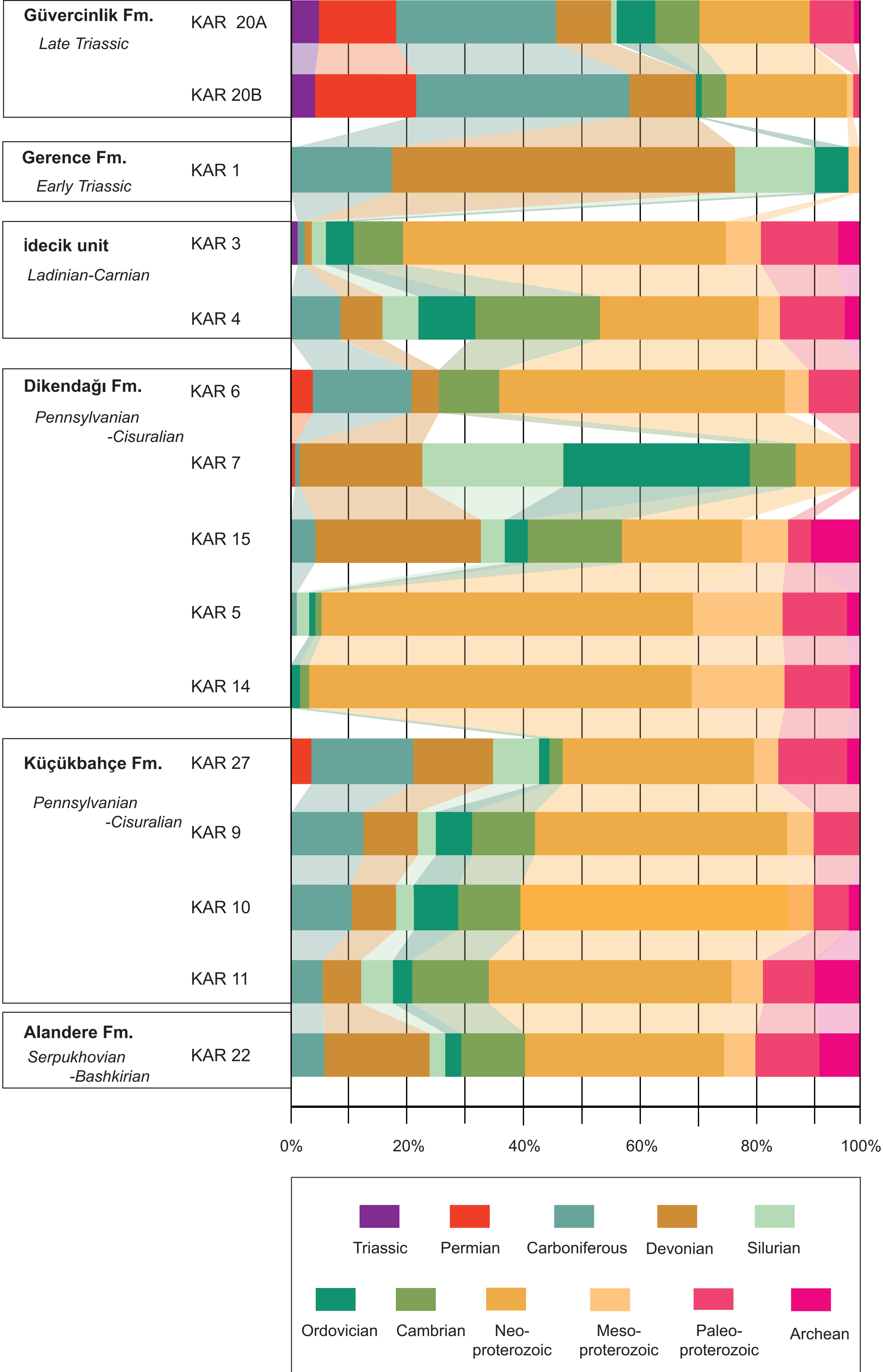

Güvercinlik Fm.
Late Triassic
KAR 20A
KAR 20B
Gerence Fm.
Early Triassic
KAR 1
idecik unit
Ladinian-Carnian
KAR 3
KAR 4
Dikendağı Fm.
Pennsylvanian
-Cisuralian
KAR 6
KAR 7
KAR 15
KAR 5
KAR 14
Küçükbahçe Fm.
Pennsylvanian
-Cisuralian
KAR 27
KAR 9
KAR 10
KAR 11
Alandere Fm.
Serpukhovian
-Bashkirian
KAR 22
0%
20%
40%
60%
80%
100%
Triassic
Permian
Carboniferous
Devonian
Silurian
Ordovician
Cambrian
Neo-
proterozoic
Meso-
proterozoic
Paleo-
proterozoic
Archean

Figure12

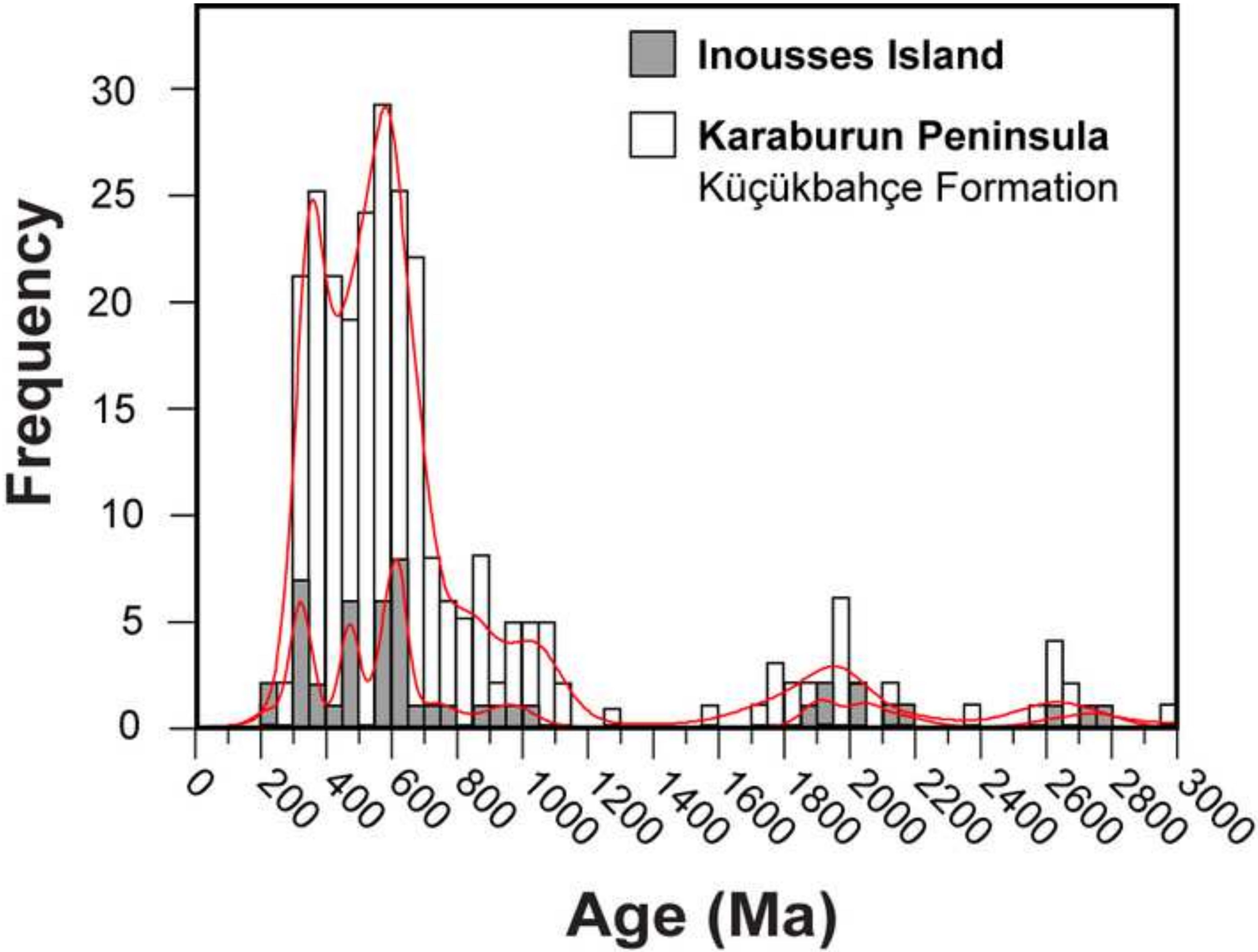

Inousses Island
Karaburun Peninsula
Küçükbahçe Formation
Frequency
30
25
20
15
10
5
0
0
200
400
600
800
1000
1200
1400
1600
1800
2000
2200
2400
2600
2800
3000
Age (Ma)

Figure13

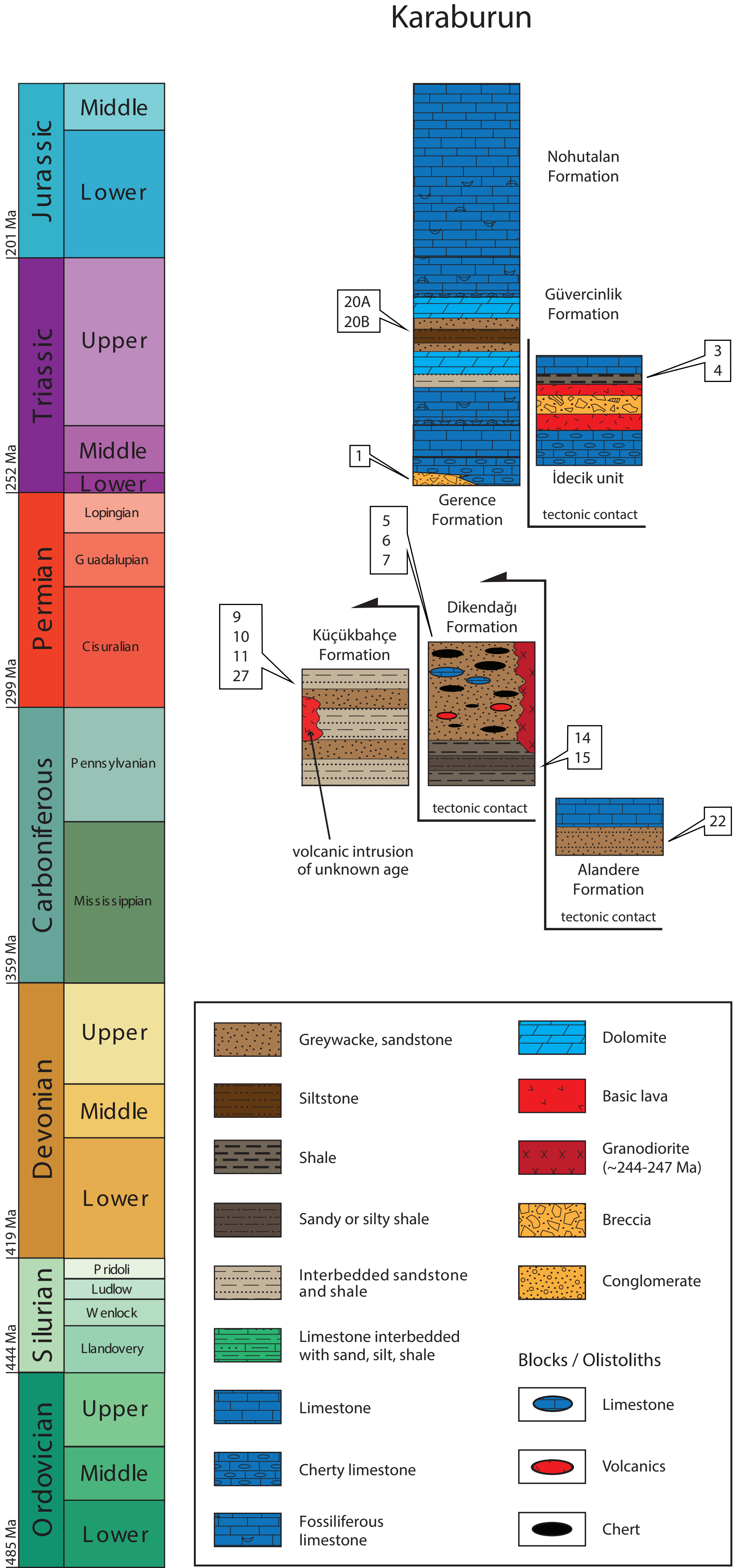

Karaburun
Jurassic
Middle
Lower
201 Ma
Triassic
Upper
Middle
Lower
252 Ma
Permian
Lopingian
Guadalupian
Cisuralian
299 Ma
Carboniferous
Pennsylvanian
Mississippian
359 Ma
Devonian
Upper
Middle
Lower
419 Ma
Silurian
Pridoli
Ludlow
Wenlock
Llandovery
444 Ma
Ordovician
Upper
Middle
Lower
485 Ma
Nohutalan Formation
Güvercinlik Formation
20A
20B
3
4
1
İdecik unit
Gerence Formation
tectonic contact
5
6
7
Dikendağı Formation
9
10
11
27
Küçükbahçe Formation
14
15
tectonic contact
22
Alandere Formation
tectonic contact
volcanic intrusion of unknown age
Greywacke, sandstone
Dolomite
Siltstone
Basic lava
Shale
Granodiorite (~244-247 Ma)
Sandy or silty shale
Breccia
Interbedded sandstone and shale
Conglomerate
Limestone interbedded with sand, silt, shale
Blocks / Olistoliths
Limestone
Limestone
Cherty limestone
Volcanics
Fossiliferous limestone
Chert

Figure14

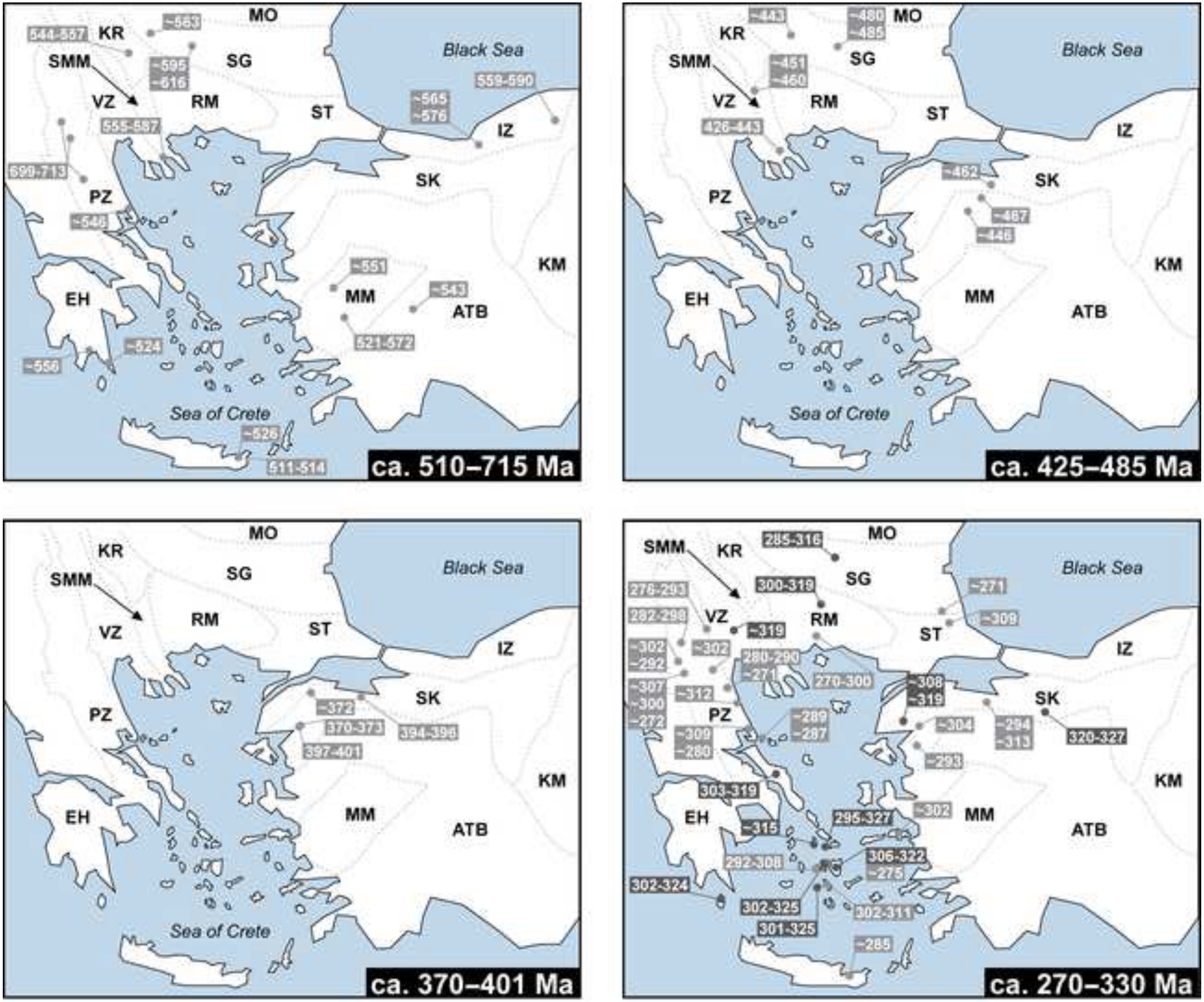
MO
KR
SMM
SG
VZ
RM
ST
Black Sea
IZ
SK
PZ
EH
MM
ATB
KM
Sea of Crete
544-557
~563
~595
~616
555-587
699-713
~546
~565
~576
559-590
~551
~543
521-572
~524
~556
~526
511-514
ca. 510–715 Ma
~443
~480
~485
~451
~460
426-443
~462
~467
~446
ca. 425–485 Ma
~372
370-373
394-396
397-401
ca. 370–401 Ma
285-316
300-318
276-293
282-298
~319
~302
~292
~307
~300
~272
~312
280-290
~271
270-300
~308
~319
~289
~287
~309
~280
~304
~293
~294
~313
320-327
~309
303-319
296-327
~302
~315
292-308
306-322
~275
302-324
302-325
302-311
301-325
~285
ca. 270–330 Ma

Figure15

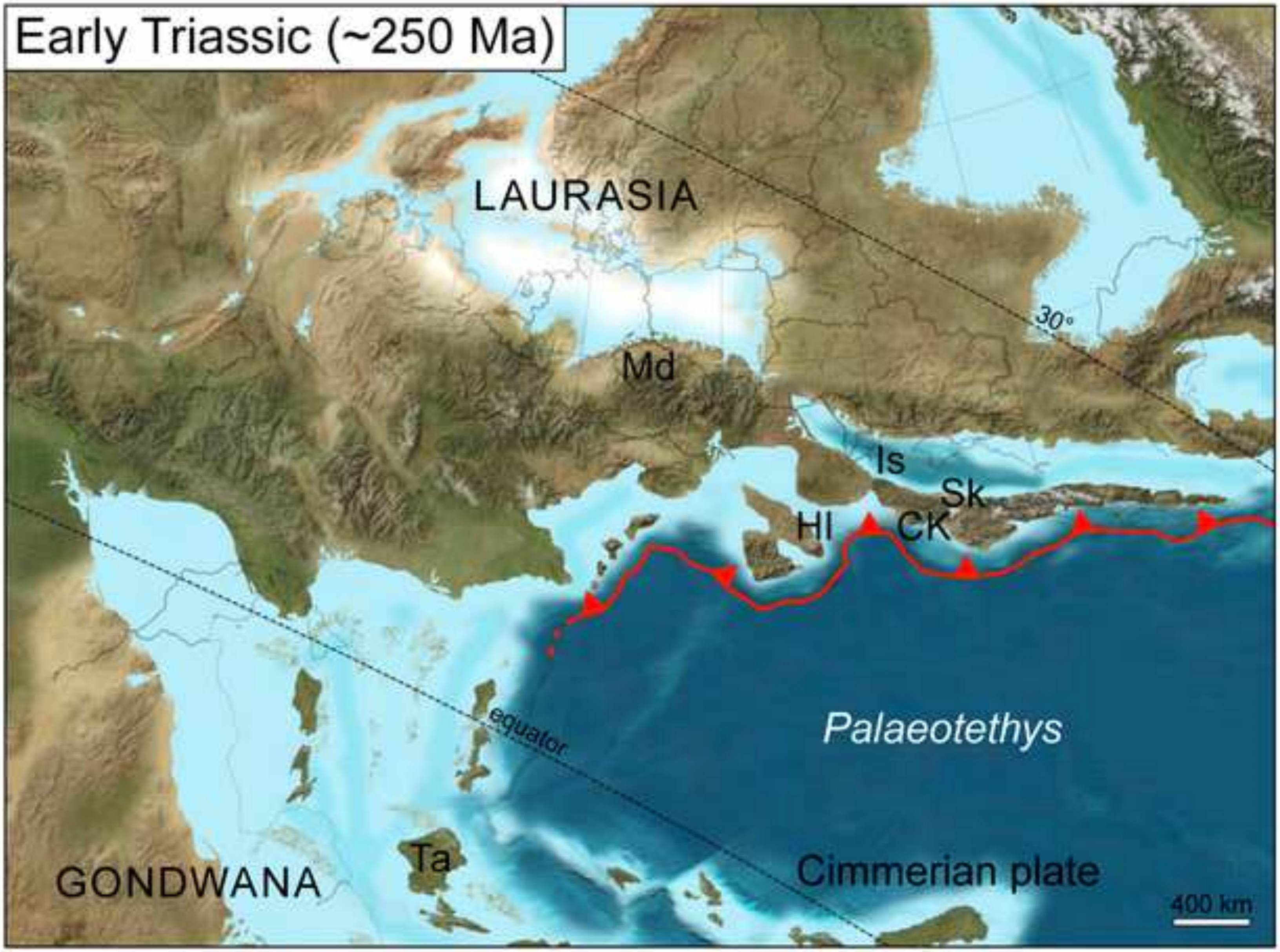

Early Triassic (~250 Ma)
LAURASIA
30°
Md
Is
Sk
Hl
CK
Palaeotethys
equator
Ta
GONDWANA
Cimmerian plate
400 km

Table 1

Sample	Lithology	Latitude	Longitude	Stratigraphic age according to fossils	Maximum depositional age according to zircon ages	accepted in this study
Güvercinlik Formation				*Late Triassic*		*Late Triassic*
KAR20A	quartz arenite	38°27'51.56"	26°35'23.41"		Late Triassic	
KAR20B	sublitharenite	38°27'51.56"	26°35'23.41"		Late Triassic	
Gerence Formation				*Early Triassic*		*Early Triassic*
KAR1	litharenite	38°26'41.44"	26°30'08.24"		Late Carboniferous	
İdecik unit				*Ladinian–Carnian*		*Ladinian–Carnian*
KAR3	sublitharenite	38°27'39.21"	26°28'37.59"		Late Ordovician	
KAR4	litharenite	38°28'24.21"	26°28'23.18"		Late Carboniferous	
Dikendağı Formation				*no record*		*Pennsylvanian–Cisuralian*
KAR5	sublitharenite	38°29'39.03"	26°27'16.20"		Early Cambrian	
KAR6	sublitharenite	38°29'14.58"	26°25'57.37"		Pennsylvanian–Cisuralian	
KAR7	lithic arkose	38°30'31.44"	26°24'17.82"		Late Devonian	
KAR14	subarkose	38°39'25.02"	26°27'32.04"		Ediacaran	
KAR15	quartz arenite	38°38'00.70"	26°27'21.10"		Early Carboniferous	
Küçükbahçe Formation				*no record*		*Pennsylvanian–Cisuralian*
KAR9	sublitharenite	38°33'48.12"	26°22'51.24"		Late Carboniferous	
KAR10	subarkose	38°36'44.64"	26°23'40.18"		Pennsylvanian–Cisuralian	
KAR11	feldspathic litharenite	38°39'43.73"	26°24'27.59"		Mid–Carboniferous	
KAR27	sublitharenite	38°38'07.78"	26°26'34.40"		Late Carboniferous	
Alandere Formation				*Serpukhovian–Bashkirian*		*Serpukhovian–Bashkirian*
KAR22	subarkose	38°24'05.34"	26°29'43.62"		Mississippian	